ANNULAR GAS SEALS AND ROTORDYNAMICS OF COMPRESSORS AND TURBINES

by
Dara W. Childs
Leland T. Jordan Professor
and
John M. Vance
Professor
Department of Mechanical Engineering
Texas A&M University
College Station, Texas

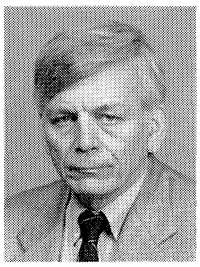

Dara W. Childs has been Director of the Turbomachinery Laboratory since 1984. He holds the Leland T. Jordan chair in Mechanical Engineering at Texas A&M University. He received his B.S. (1961) and M.S. (1962) degrees (Civil Engineering) from Oklahoma State University, and his Ph.D. (Engineering Mechanics) from the University of Texas (1968).

Dr. Childs' expertise is in the area of dynamics and vibrations, with an emphasis in the area of rotordynamics. He has conducted research and engineering projects for NASA, DOD, and private firms related to rotordynamics.

Dr. Childs is the author of numerous reviewed publications related to rotordynamics and vibrations, and author of the book, Turbomachinery Rotordynamics. *He is currently carrying out tests on honeycomb and hole-pattern gas damper seals for a 12-member industrial consortium. He was named an ASME Fellow Member in 1990, and received ASME's Henry R. Worthington Medal in 1991.*

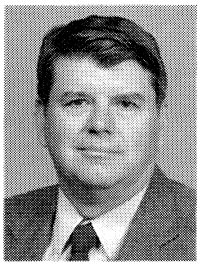

John M. Vance is Professor of Mechanical Engineering at Texas A&M University. He received his B.S. (Mechanical Engineering) (1960), M.S. (Mechanical Engineering) (1964), and Ph.D. (1967) degrees from the University of Texas.

Prior to joining Texas A&M (1978), Dr. Vance held positions at Armco Steel, Texaco Research, and Tracor, Incorporated, and developed a Rotordynamics Laboratory at the University of Florida. He is currently conducting research on rotordynamics, damper seals, and bearing dampers. He has published a book Rotordynamics of Turbomachinery *(John Wiley, 1988) and more than 50 technical articles and reports. Dr. Vance is consultant to industry and government and has held numerous summer appointments. He organized the annual short course for industry at Texas A&M on "Rotordynamics of Turbomachinery" and co-organized the biennial "Workshop on Rotordynamics Instability Problems in High Performance Turbomachinery." Dr. Vance is a member of ASME and ASEE, and is a registered Professional Engineer in the State of Texas.*

ABSTRACT

The possible negative or positive impact of annular seal on rotordynamics of compressors and steam turbines is discussed. The nature of destabilizing forces that can be developed by "see-through" and interlocking labyrinths is discussed. Improving the rotordynamic behavior of labyrinths via swirl brakes and shunt injection is explained using measured test results. Improving rotordynamics through replacement of labyrinths with either smooth-rotor/honeycomb-stator seals (honeycomb seals) or pocket damper seals is also discussed. For long seals (L > 2 in or 50 mm) honeycomb seals leak about a third less than a standard labyrinth, have much higher values of effective damping, and potentially high stiffness values for high-pressure compressors. The pocket damper seal is a patented device with damping values that can be a hundred times higher than a standard labyrinth seal. Recent test results are presented for both seal types, and case studies are cited and reviewed where unstable compressors have been "cured" through application of these seals.

INTRODUCTION

The first task of an annular seal is the restriction of leakage flowrate between a rotating shaft and a stationary housing. As it turns out, annular gas seals can also have a significant impact on dynamic characteristics of compressors and turbines. Hence, at the outset of this study, the types and functions of seals will be considered, in addition to their dynamic characteristics.

The forces developed by gas seals are roughly proportional to the pressure differential (ΔP) across the seals and the fluid density within the seal. Because of the density dependency, gas seals have a greater impact on the rotordynamics of steam turbines and high-pressure compressors where densities are higher than on gas turbines. In the case of the TAMSEAL™ (a new type of pocket damper seal [1]), the dependence on ΔP is greater, and the dependence on density is weaker.

Seal Configurations and Functions

High pressure compressors can use either the "flow-through" or "back-to-back" designs of Figure 1. In the through-flow design, gas enters from the left and proceeds directly from impeller to impeller, discharging on the right. For the back-to-back design, flow enters at the left and proceeds from left to right through the first four stages, then follows a crossover duct to the right hand side of the machine, and proceeds from right to left through the last four stages, discharging at the center. Back-to-back machines obviously produce a smaller axial thrust than flow-through or series machines.

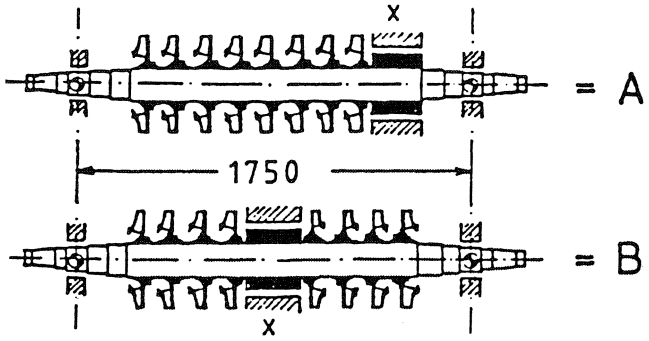

Figure 1. (A) Flow-through or Series and (B) Back-to-Back or Parallel Compressor Designs [2].

A typical sealing arrangement for a last stage compressor impeller is illustrated in Figure 2. The eye packing seal limits return-flow leakage down the front of the impeller, and the shaft seal restricts return-flow leakage along the shaft to the preceding stage.

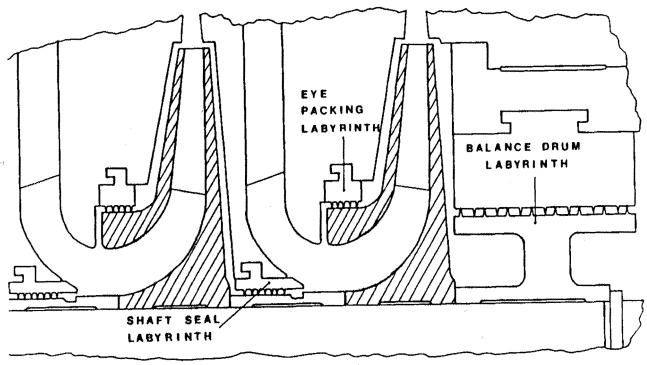

Figure 2. Typical Impeller Seal Arrangement for the Last Stage of a Centrifugal Compressor [3].

In a series compressor, leakage flow through the balance drum is returned to the inlet; hence, the balance drum absorbs the full ΔP of the compressor, and the fluid within the seal has an average density that is approximately proportional to the average of inlet and discharge pressures. For a back-to-back machine, the balance drum absorbs the ΔP between the last stage of the compressor and the last stage of the initial series of impellers, i.e., about one half of compressor ΔP. For the same inlet and discharge pressures, the *average* density is higher in the center seal of a back-to-back machine than in the balance-drum seal of a series machine. For a series machine, pressure ratios across a balance drum are on the order of 0.4 to 0.5 *vs* 0.6 for the center seal of a back-to-back machine. Note that the flow for a balance-drum seal proceeds radially inwards along the back side of the impeller before entering the seal. Historically, back-to-back compressors are more sensitive to the forces from the central seal than are series machines to forces from the balance-drum seal. This result would be expected because of the customary rotor first critical speed modeshape, with a much larger amplitude at a center seal in the middle of the rotor than a balance-piston seal located toward the rotor's end.

The balance drum seal design of Figure 2 is said to be an "interlocking" or full labyrinth design. The stator portion of the seal is split diametrically and fitted around the shaft with a radial interference that limits relative axial motion of the rotor and stator. The eye packing and shaft seals are called "see-through" or "half" labyrinth. These seals in Figure 2 have the teeth on the stator (TOS), which is typical of compressors; however, turbines normally have the teeth on the rotor (TOR).

"Abradable" labyrinth seals are a variation of teeth-on-rotor labyrinths for which a soft material is used on the stator. The seals are assembled with a tight but finite clearance. As the shaft speed increases, centrifugally-induced stresses cause the rotor to grow, and the teeth eventually cut into the stator, creating an interference fit and significantly reducing leakage. Abradable seals have been used for many years in aircraft gas turbines, with the stator element being made from honeycomb (Figure 4) or powdered-metal composites. Various plastics have been used for abradable-seal liners in commercial turbomachinery [4, 5].

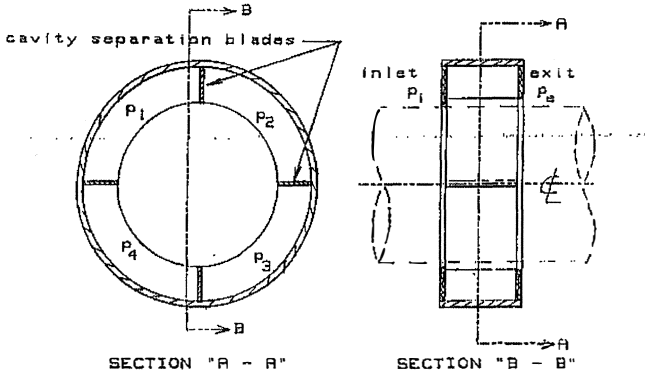

Figure 3. Single-Cavity Pocket Damper Seal [1].

Illustrated in Figure 3 is a single-cavity pocket damper seal. This labyrinth seal was developed by Vance and Schultz [1] and incorporates the following two critical elements:

- The seal diverges axially; i.e., the exit-tooth clearance is larger than the inlet-tooth clearance.
- Webs are installed in the labyrinth cavity to reduce or eliminate circumferential flow, and to create pressure pockets.

The pocket damper seal has much higher damping than conventional labyrinths and has been used to eliminate instability problems in a range of centrifugal compressors.

Illustrated in Figure 4 is a smooth-rotor/honeycomb stator seal. The honeycomb surface is brazed into an outer bore. The rough outer surface acts to reduce the leakage. At the same radial clearance, honeycomb seals leak significantly less than see-through labyrinth seals. Recent test results and experiences with numerous unstable compressors and one published account for a steam turbine demonstrate excellent rotordynamic characteristics for this type of seal.

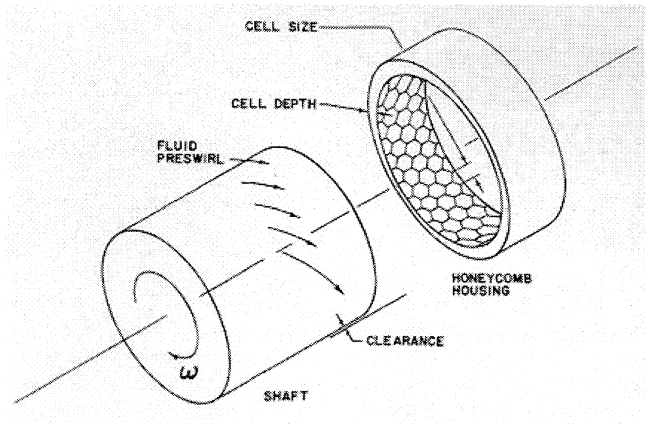

Figure 4. Smooth-Rotor/Honeycomb-Stator Seal [6].

Illustrated in Figure 5 are two "floating-ring" bushing seals used in a high pressure oxygen turbopump (HPOTP) of the space shuttle main engine (SSME). The bushings are made from carbon, have a smooth inner surface, and a convergent taper seal geometry. The seals are

designed to be self centering at low ΔP readings and to "lockup" at higher ΔP readings. Very tight clearances are generally used for bushing seals. This seal type is sometimes used on geared compressors.

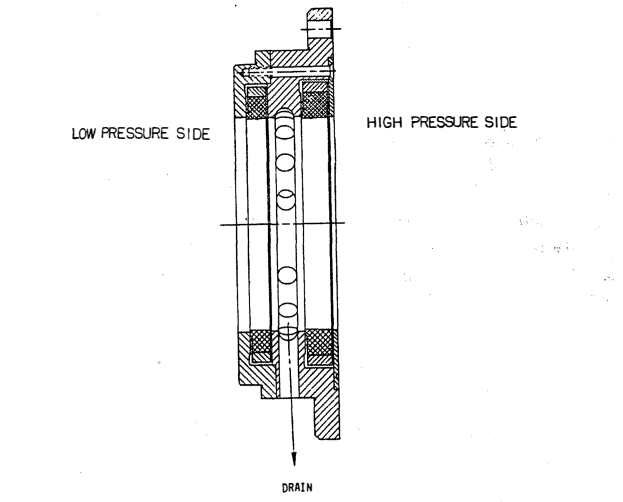

Figure 5. Floating-Ring Gas Seal [6].

A "brush" seal is illustrated in Figure 6. This seal uses a biased pattern of wires in contact with a ceramic coating on the shaft and has a sharply reduced leakage flow, as compared to a labyrinth or honeycomb seal. Based on initial tests, the brush seal has favorable rotordynamic characteristics as compared to labyrinth configurations. These seals are used heavily in new aircraft gas turbines because of their exceptionally good leakage performance. They are also being pursued for industrial gas turbines [7].

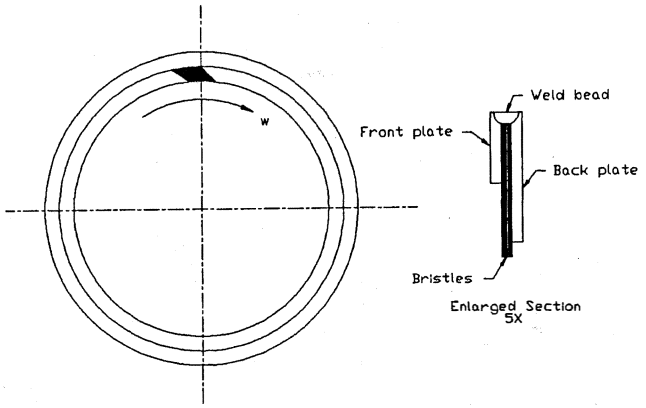

Figure 6. Brush-Seal Configuration [6].

Illustrated in Figure 7 is the leakage path for a high pressure steam turbine. Labyrinth seals are customarily applied at the interstage diaphragm, and inlet and exit shaft locations.

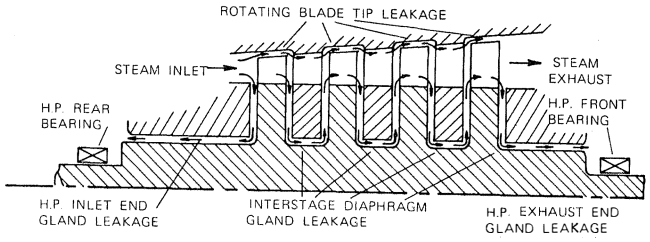

Figure 7. Steam Turbine Seal Path [8].

The rotordynamic characteristics of each seal type introduced are discussed further in the balance of this study, with particular emphasis on seals that can either significantly improve or significantly degrade rotordynamic characteristics of turbomachinery. The next subsection will consider characteristics of unstable turbomachinery, review some early test results for gas seals, and introduce the customary rotordynamic model used for seal reaction force components.

Initial Rotordynamic Instability Experiences And Test Results for Annular Gas Seals

Experience has shown that annular seals can have a significant impact on the rotordynamic characteristics of high-pressure centrifugal compressors and steam turbines, particularly in regard to their stability characteristics. Early instability experiences with centrifugal compressors were characterized by *onset-load* or *power* limits *vs onset-speed* limits for rotors operating on fixed-arc hydrodynamic bearings. These power-limiting instability cases typically occurred with rotors operating on tilting-pad bearings; hence, although the units were operating at speeds in excess of twice their first critical speeds, there was no basis for believing that the bearings were causing the instability. Notable case studies documenting early compressor instabilities are provided in the literature [9, 10]. Most of the initial compressor problems were resolved by increasing the rotor critical speed through direct stiffening of the rotor and/or shortening the bearing span.

Illustrated in Figure 8 is a vibration spectrum for an unstable five-stage, straight-through, hydrogen-recycle compressor. The rotor is running at 8475 rpm on five-shoe, load-on-pad tilting-pad bearings. The unstable response is at the rotor's natural frequency ω_n of 412 rpm. In Figure 8, the synchronous response amplitude at 8475 rpm is larger than the subsynchronous response at 4125 rpm; however, in many cases, as power or ΔP is increased, the subsynchronous response dwarfs the synchronous component. Figure 9 illustrates how the subsynchronous component can increase with increasing ΔP. For synchronous motion, the rotor is excited by imbalance and precesses at running speed; i.e., the rotor traces out an orbit with period $2\pi/\omega$. For unstable motion, the rotor precesses simultaneously at both running speed ω and the rotor natural frequency ω_n.

Very similar instability problems were reported for steam turbines. Pollman and Termeuhlen [12] cited load-dependent cases of "steam whirl." Some steam-whirl cases appear to be load dependent but are, in fact, caused by fixed-arc hydrodynamic bearings during partial-arc-admission to the turbine. Under these conditions, a bearing can be unloaded, causing an oil-whip/oil-whirl instability. However, Pollman and Termeuhlen [12] and Greathead and Bostow [8] present load-dependent cases for which the instability was clearly not caused by unloading the bearings. Many cases of steam whirl are simply accommodated by operating the turbine at reduced power settings *vs* eliminating the instability problem.

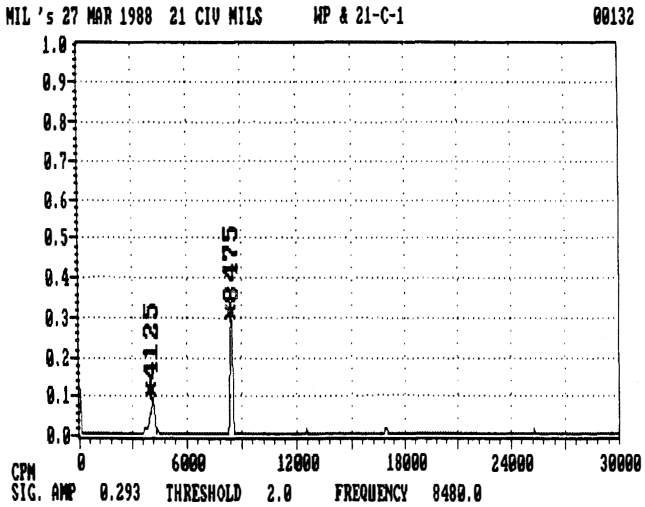

Figure 8. Spectrum for an Unstable Hydrogen-Recycle Compressor [11].

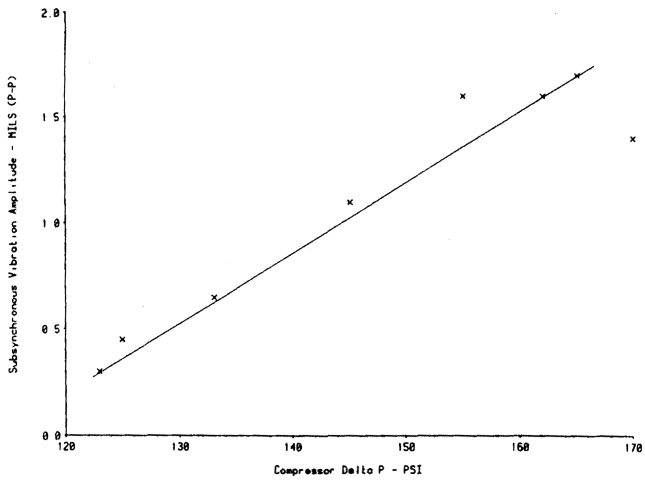

Figure 9. Subsynchronous Vibration Amplitude vs *ΔP for a Hydrogen-Recycle Compressor [11].*

The analysis of Thomas [13] and Alford [14] provided a possible explanation for instabilities in steam turbines. Their model is stated:

$$-\begin{Bmatrix} F_X \\ F_Y \end{Bmatrix} = \begin{bmatrix} 0 & k_q \\ -k_q & 0 \end{bmatrix} \begin{Bmatrix} X \\ Y \end{Bmatrix} \tag{1}$$

where F_X, F_Y and X, Y are, respectively, components of the reaction force and rotor displacement vector, and k_q is a destabilizing cross coupled stiffness coefficient defined by:

$$k_q = \frac{T\beta}{D_m L_t} \tag{2}$$

In this definition, T is the turbine-stage torque, D_m is the mean diameter of the turbine blades, L_t is the turbine-blade length, and ß is defined by Alford [14] as, "the change in thermodynamic efficiency per unit of rotor displacement, expressed as a fraction of blade height." The clearance-excitation model of Equations (1) and (2) arises because of the change in turbine-blade efficiency with a change in clearance, but there is no *physical* basis for a comparable shrouded-impeller model in centrifugal compressors.

In the absence of a good explanation for load-dependent instabilities in centrifugal compressors, German researchers began to investigate labyrinth seals as a cause of rotordynamic instability. Employing the stiffness model:

$$-\begin{Bmatrix} F_X \\ F_Y \end{Bmatrix} = \begin{bmatrix} K & k \\ -k & K \end{bmatrix} \begin{Bmatrix} X \\ Y \end{Bmatrix} \tag{3}$$

Benckert and Wachter [2, 15] measured direct K and cross coupled *k* stiffness coefficients for a wide range of see-through and interlocking labyrinth geometries. Their test procedure involved displacing the rotor in the X direction a distance e_0 and measuring the resulting circumferential pressure distribution in labyrinth cavities. Integrating the perturbed pressures yields a reaction force component in the direction of displacement, $-Ke_0$, and the component ke_0 perpendicular to the displacement direction. The following two types of tests were performed:

- Air entering the seal was preswirled while the rotor was stationary (not rotating).
- Air entered a rotating seal without preswirl.

Tests showed that the direct stiffness coefficient K is negligible, but *the cross coupled stiffness coefficient k is significant and arises due to the circumferential velocity of gas entering the seal or developed within the labyrinth cavities due to shaft rotation.* With the insight that fluid rotation caused the destabilizing forces, Benckert and Wachter [2, 15] developed "swirl brakes" to destroy or reduce preswirl entering a labyrinth. Figure 10 shows the measured destabilizing force increasing as the static eccentricity increases. The slope of the force *vs* eccentricity line defines k. Note that adding webs decreases k, and that introducing eight swirl webs upstream of the labyrinth actually changes the sign of the lateral force component. Swirl-brake technology was rapidly implemented into compressors of several German and Swiss manufacturers, substantially improving their stability characteristics. Some recent experiences with swirl brakes are discussed further below.

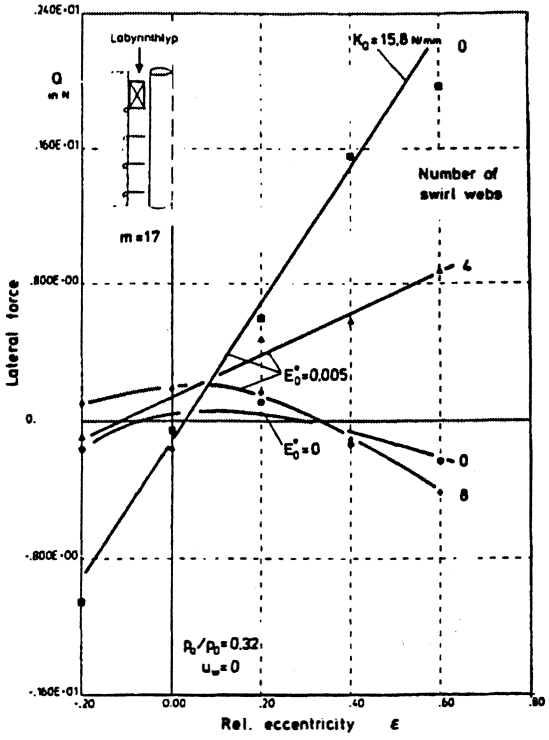

Figure 10. Reduction of Seal Cross Coupled Stiffness Force by Placing Swirl Webs Immediately Upstream of a Labyrinth [2]; 17 Labyrinth Chambers.

Illustrated in Figure 11 is the influence of various levels of preswirl and the influence of changing the direction of fluid prerotation. In Figure 11, U_w is the preswirl velocity. Benckert and Wachter [2, 15] held the preswirl direction constant and changed the direction of shaft rotation to obtain prerotation against rotation. Clearly, increasing the circumferential velocity in the direction of rotation increases k, and reversing the preswirl *changes the sign of k.* Similar results are shown in Figure 12 [16] for:

- Smooth constant-clearance
- TOS labyrinth
- Smooth-rotor/honeycomb-stator seal designs

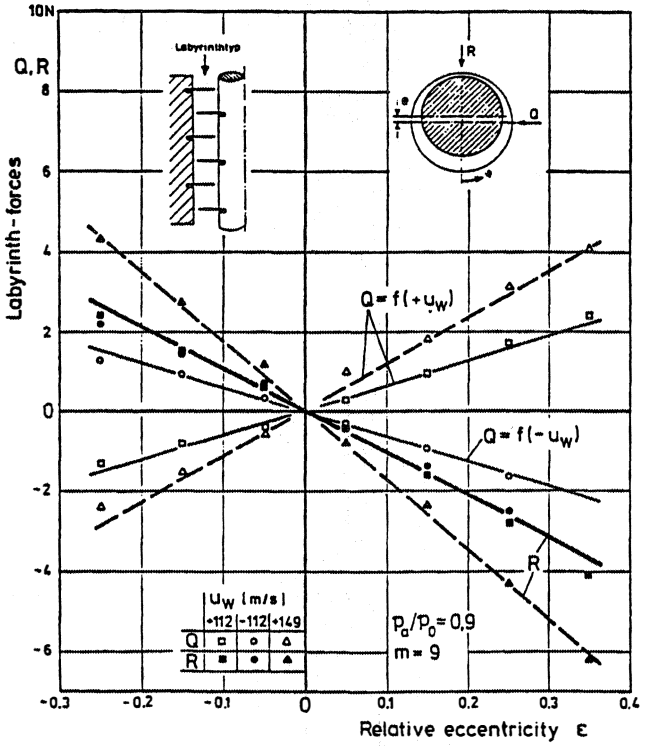

Figure 11. The Influence of Prerotation (Positive and Negative) on k *[15].*

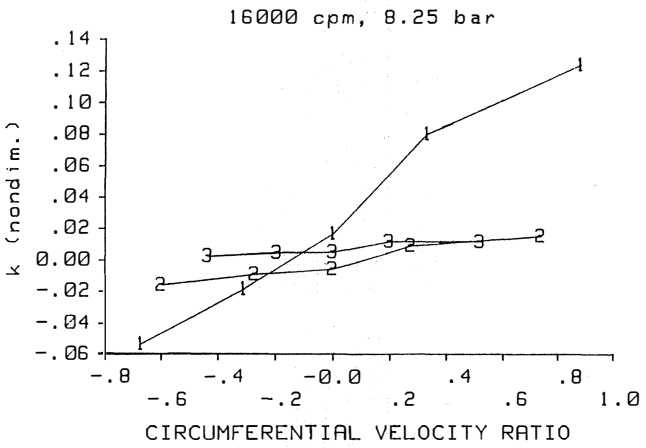

Figure 12. k (Nondimensional) vs *Preswirl for: (1) Smooth Constant-Clearance, (2) TOS Labyrinth, and (3) Smooth Rotor/Honeycomb-Stator Designs [16].*

The "natural" level of preswirl in a compressor seal varies considerably with its function. The eyepacking labyrinth of Figure 2 has a high degree of preswirl, because the gas that it seals leaves the impeller with a substantial circumferential velocity in the direction of rotation, and, typically, accelerates as it proceeds radially inward along the impeller. A similar situation holds for the balance-drum seal. Conversely, in most cases the flow entering shaft seals has negligible prerotation. The inlet circumferential velocity ratio:

$$u_0(0) = U_0(0)/R\omega \tag{4}$$

is the inlet gas circumferential velocity, divided by the adjacent rotor surface velocity. For eyepacking or balance drums, this ratio can reach 0.8; for shaft seals, values on the order of 0.1 are more appropriate.

To fully appreciate the consequence of *actively* reducing k or changing its sign, damping needs to be incorporated into the reaction-force model for labyrinths, yielding:

$$-\begin{Bmatrix} F_X \\ F_Y \end{Bmatrix} = \begin{bmatrix} K & k \\ -k & K \end{bmatrix} \begin{Bmatrix} X \\ Y \end{Bmatrix} + \begin{bmatrix} C & c \\ -c & C \end{bmatrix} \begin{Bmatrix} \dot{X} \\ \dot{Y} \end{Bmatrix} \tag{5}$$

where C and c are the direct and cross coupled damping coefficients, respectively.

The radial and circumferential force components of the seal reaction force modelled by Equation (5) are illustrated in Figure 13, with a synchronous precession orbit of radius A. (By synchronous, we mean that the precessional frequency Ω is the same as the spin speed ω.) The radial force component, $F_r = -(K + c\omega)A$ is negligible for *labyrinth* seals. The circumferential force term, $F_\theta = (k - C\omega)A$, can either destabilize ($F_\theta > 0$) or stabilize ($F_\theta < 0$) a rotor in forward whirl.

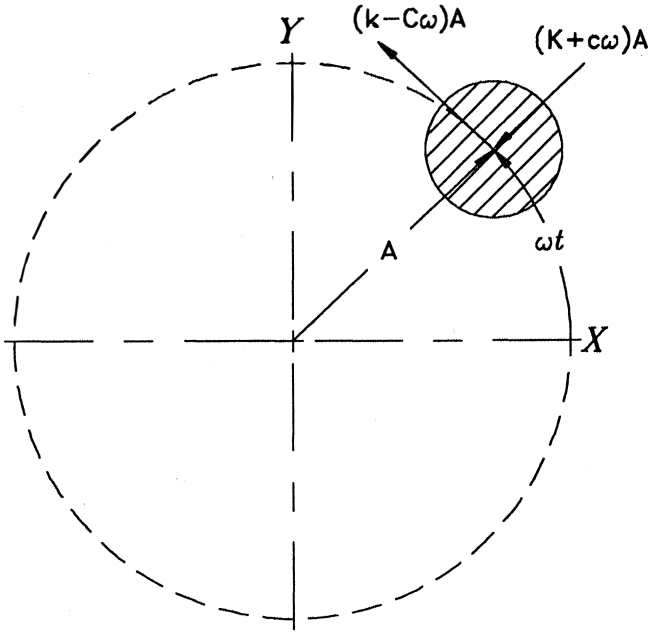

Figure 13. Precessing Seal with Radial and Circumferential Force Components.

A forward-whirl instability of a rotor occurs when the rotor is precessing at its natural frequency in the direction of shaft spin rotation. Except for dry-friction whip and whirl, virtually all rotordynamic instabilities are forward.

Returning to F_θ, the destabilizing and stabilizing contributions are defined, respectively, by kA and $C\omega A$. The ratio of these two components is the whirl-frequency ratio:

$$f_w = \frac{k}{C\omega} \tag{6}$$

This ratio should be minimized to enhance stability and is a very useful term for comparing the relative stability characteristics of fixed-arc hydrodynamic bearings. It is less useful in comparing the stabilizing or destabilizing characteristics of gas annular seals. A more appropriate term can be deduced from:

$$-\frac{F_\theta}{A} = C - k\omega = C\left(1 - \frac{k}{C\omega}\right)\omega = C_{eff}\omega \qquad (7)$$

Hence,

$$C_{eff} = C\left(1 - \frac{k}{C\omega}\right) = C\left(1 - f_w\right) \qquad (8)$$

When comparing two annular seals, at the same running speed and operating conditions, the "best" seal from a rotordynamic viewpoint will have the largest value for C_{eff}, and large values for C_{eff} can be obtained by increasing C and reducing, *or reversing, the sign of k.*

In the same 1965 study where Alford [14] gave Equation (2) for cross coupled stiffness due to tip clearance effects on axial flow wheels, he also hypothesized a theory to predict direct damping coefficients of labyrinth seals with two blades and choked flow. Cross coupled forces were not considered. The most notable prediction of Alford's analysis was that seals with clearances converging in the direction of flow would have negative damping coefficients ($C < 0$), and seals with diverging clearances would have positive damping coefficients ($C > 0$). The predicted coefficients are quite large. This theory, which modelled only the axial flow and neglected circumferential flow effects, was later extended to multiple blades and unchoked flow by Murphy and Vance [17]. They predicted that a ten bladed diverging labyrinth of 200 mm (7.8 in) diameter and with a pressure ratio of 10 could have a direct damping coefficient equal to 87,560 N-s/m (500 lb-s/in), which is about the same as a typical squeeze film bearing damper of similar dimensions. More than 10 years of testing labyrinth seals has shown that the direct damping coefficients of conventional labyrinth seals are, in fact, very small and never approach even a small percentage of the values predicted by Alford's theory. Instead, the dominant rotordynamic coefficient of conventional seals is cross coupled stiffness that reduces the *effective* damping and can even be destabilizing to rotor whirl. The reason for this failure of Alford's theory is that conventional labyrinth seals have continuous and unobstructed annular grooves so that pressure variations across the seal diameter cannot exist without large circumferential flowrates. Unfortunately, it is the circumferential swirl that produces the undesirable cross coupled stiffness. The pocket damper seal design of Figure 3 greatly reduces circumferential flow and makes a seal for which the direct damping predictions of Alford become much more accurate. A more rigorous analysis based on the assumption that the control volumes are unconnected around the circumference was developed and was applied first to the development of a piston operated bearing damper, Sundararajan and Vance [18]. It produces predictions for the pocket damper seals that are within 10 percent of the direct damping measurements for the two bladed version, for pressure ratios between 3.0 and 4.0.

Iwatsubo [19] made photographs through a transparent labyrinth seal wall that reveals a very complex flow pattern, containing vortices, around the annulus. The pocket damper seal design breaks up this flow and makes it of secondary importance, relative to the axial flow in and out of the cavities. This is why such a simple theory for this seal design (based on an assumption that the average pressure in the seal cavities can be calculated based on axial mass flowrates into and out of the cavities) gives fairly accurate predictions, especially for two bladed seals. For seals with more blades, it appears that the viscosity of the gas degrades the damping to some extent. A more advanced computer code is now being developed to predict the effect of viscosity of the gas and the circumferential swirl effects (if any).

Most of the investigations of labyrinth seal effects on rotordynamics have been concerned with stability. The shaft speed frequency ω in Equation (7) is used by the first author to calculate the effective damping C_{eff} of most gas seals, even though the actual whirl frequency in stability problems is asynchronous ($\Omega \neq \omega$). This is done to compare different seals on the same basis at running speed, since Ω may not be known. Furthermore, the pressure drop ΔP and the cross coupled stiffness k are usually changing with shaft speed ω. The pocket damper seal has unique characteristics, and the second author uses a different procedure. The current computer code for the seal's damping coefficients has ΔP as an input. The (usually) subsynchronous whirl frequency Ω is used in Equation (7), if it is known, since the seal has very little cross coupling, and the coefficients are independent of shaft speed, but depend on Ω. The correct value for the "effective damping" C_{eff} will then be obtained in the following sense: C_{eff} can be used as the direct damping coefficient C with $k = 0$ in a rotordynamic computer code and the logarithmic decrement will be correctly predicted.

A fact sometimes neglected is that labyrinth seals can also affect the amplitudes of synchronous response to imbalance. This can be shown in the simplest way by including cross coupled stiffness in the imbalance response analysis of a Jeffcott rotor or a short rigid rotor. The following equation for the response amplitude r is from Vance [20]:

$$r = mu\,\omega^2 / [(2K_B - m\,\omega^2)^2 - (2\,\omega C - k)^2]^{1/2} \qquad (9)$$

where mu is the rotor imbalance and K_B is the bearing stiffness. A positive cross coupled stiffness (k coefficient) can greatly increase the magnification factor of imbalance at the critical speed. But, if k is large enough relative to C, it can reduce the magnification factor (not the usual case). Note, also, that a negative value for k can reduce the magnification factor at the critical speed. This shows that the identification of system damping from measured vibration response plots is really an identification of direct damping and cross coupled stiffness combined.

Experimental measurements of the effect of labyrinth seals on imbalance response were reported by Vance, et al. [21]. Straight-through labyrinth seals were installed in a rotordynamic rig instrumented for coastdown measurements of imbalance response (Bodé plots). Both teeth-on-rotor and teeth on stator gas seals were tested, each with twelve blades, 173 mm (6.81 in) blade diameter and 102 mm (4.11 in) total length. The nominal blade tip clearance was 0.5 mm (20 mils). The teeth on stator seal was tested with the blade tip clearances diverging (in the direction of flow), uniform and converging. The teeth-on-rotor seal was tested with uniform clearances. The inlet air pressure to the seals was varied from 1.7 bar to 14.6 bar (25 to 200 psig) with the last blade exhausting to the atmosphere. There was no preswirl. Coastdown tests of all the seals were performed on a rotordynamic test rig to show their effect on synchronous response to imbalance when passing through a 3700 rpm critical speed. The synchronous response to imbalance was generally increased by all the seals at inlet pressures up to about 11.2 bar (150 psig). The worst case was for the teeth-on-rotor seal at about 2.7 bar (35-45 psi) inlet pressure where the rotor whirl amplitude was increased from 0.1 mm (3.75 mils, peak-to-peak) to over 0.13 mm (5 mils). In most cases, the rotor whirl amplitude was slightly decreased at inlet pressures above 13 bar (176 psig). How the peak responses of both seals varied with the upstream pressure is shown in Figure 14. Rap testing showed that the seals actually had a small amount of positive damping at zero speed, so it is reasonable to assume that the swirl induced by spin of the rotor decreased the effective damping and made it negative in some cases.

Figure 15 illustrates "shunt injection" against rotation in a centrifugal compressor. With this approach, high pressure gas is taken from the diffuser of the last compressor stage and injected into the upstream portion of the balance-piston seal in

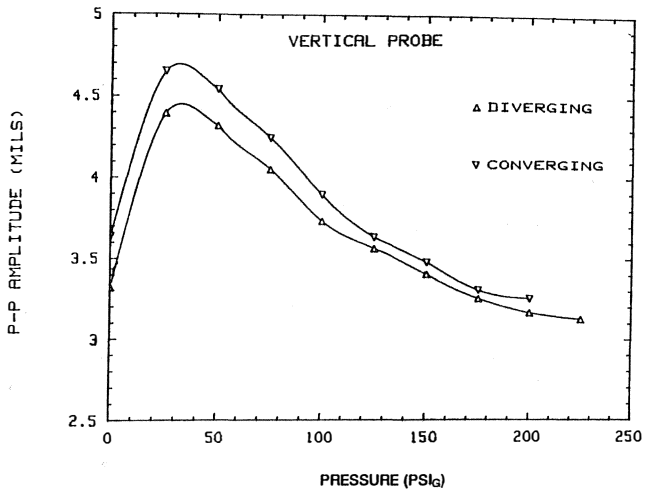

Figure 14. Peak Response, with Converging and Diverging Labyrinth Seals, vs *Pressure.*

a direction opposed to shaft rotation. (Some compressor manufacturers use radially-directed shunt injection.) Since the injection pressure is higher than the impeller discharge pressure, part of the injected gas moves "upstream," out through the "inlet" of the seal, and radially outwards along the back side of the impeller. Radial injection gives a reduction in k, and injection against rotation can yield negative values for k and increased magnitudes for C_{eff}. Recent test results for seals using radial and against-rotation shunt injection are discussed below.

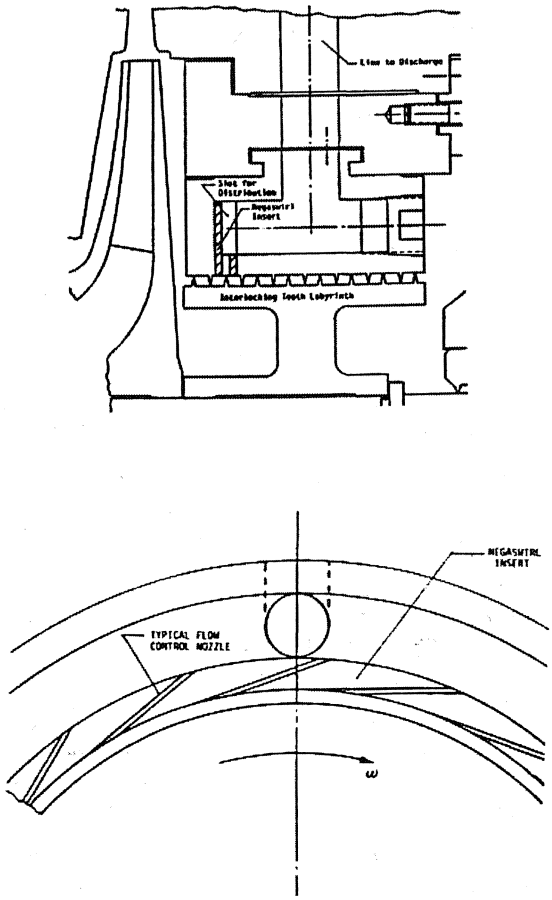

Figure 15. Against-Rotation Shunt Injection for a Balance-Piston Seal in a Through-Flow Compressor [22].

As noted previously, Benckert and Wachter [2, 15] only measured stiffness coefficients, and their comparison of cross coupled stiffness coefficients for labyrinths and smooth-rotor/honeycomb-stator seals are provided in Figure 16. The obvious (and erroneous) conclusion from Figure 16 is that honeycomb-stator/smooth-rotor seals should not be used, because of their high values of cross coupled stiffness. The missing information from Figure 16 concerns damping. Honeycomb seals typically have much higher direct damping values than labyrinths, yielding much higher values for C_{eff}. Instabilities have been eliminated in several compressors by replacing labyrinth seals with honeycomb seals, and the nature, application, and character of this seal type are discussed at length below.

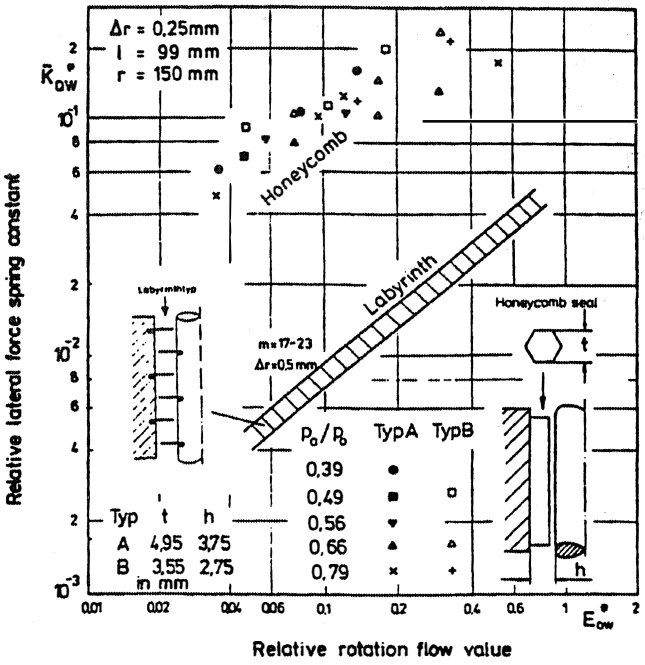

Figure 16. k for Smooth-Rotor/Honeycomb-Stator and Labyrinth Seals [2].

One of the perennial questions concerning annular gas seals and rotordynamics is: *These forces do not look very big compared to the bearings. How can they make much difference in rotor response or stability?* It is true that gas annular seals generally have small radial forces that do not significantly influence critical-speed locations. (*Note*: some recent results suggest that honeycomb/stator/smooth-rotor seals can develop large, frequency-dependent stiffnesses. This point is discussed further, later.) However, their circumferential force components can have a significant impact on stability and peak response. At the onset of instability, the circumferential components of the many forces acting on a rotor are roughly in equilibrium, and any additional stabilizing circumferential forces may be enough to stabilize an otherwise unstable rotor. Alternatively, the elimination of even a small destabilizing force in the circumferential direction may be enough to induce stability. Peak rotor response amplitudes during a critical-speed transition are similarly sensitive to damping levels; hence, elimination or reduction of a destabilizing cross coupled-stiffness coefficient or addition of comparatively small damping levels can significantly reduce peak rotor-response levels at the critical speed.

An additional reason why seals can have a major impact on the stability and response amplitudes during a critical speed transition has to do with their location on the rotor and their relative amplitude in the rotor's first-natural-frequency mode shape. To be specific, seals are generally located toward the center of the rotor

and have large modal amplitudes in comparison to bearing locations. From a modal viewpoint, the effectiveness of a load element (bearing, seal, etc.) is approximately proportional to the square of its modal amplitude. Hence, an annular seal located in the middle of a rotor can have an (apparently) disproportionate impact on both stability and peak-amplitude response during a critical-speed transition.

SEALS THAT CAUSE ROTOR STABILITY PROBLEMS

Interlocking and see-through labyrinth seals are frequent troublemakers in compressors and turbines. For compressors, eye-packing and balance-piston seals create the largest destabilizing forces because of the highly prerotated flow entering these seals. The dependency of k on inlet circumferential velocity ratio for an eight-cavity TOS seal is shown in Figure 17. The seal had a six inch (152.4 mm) diameter, a length of one inch (25.4 mm), and clearance-to-radius ratio of 0.003. Data are provided for three running speeds, three supply pressures, and three pressure ratios. The results basically confirm Wachter and Benckert's [2, 15] measurements for cross coupled stiffness coefficients. Measured values for direct-damping coefficients from Pelletti [22] show small but significant damping levels. Illustrated in Figure 18 is f_w, which combines the effect of k and C, for the labyrinth of Figure 17, with three clearances. Observe that f_w increases with increasing pressure ratio (decreasing ΔP, but higher density).

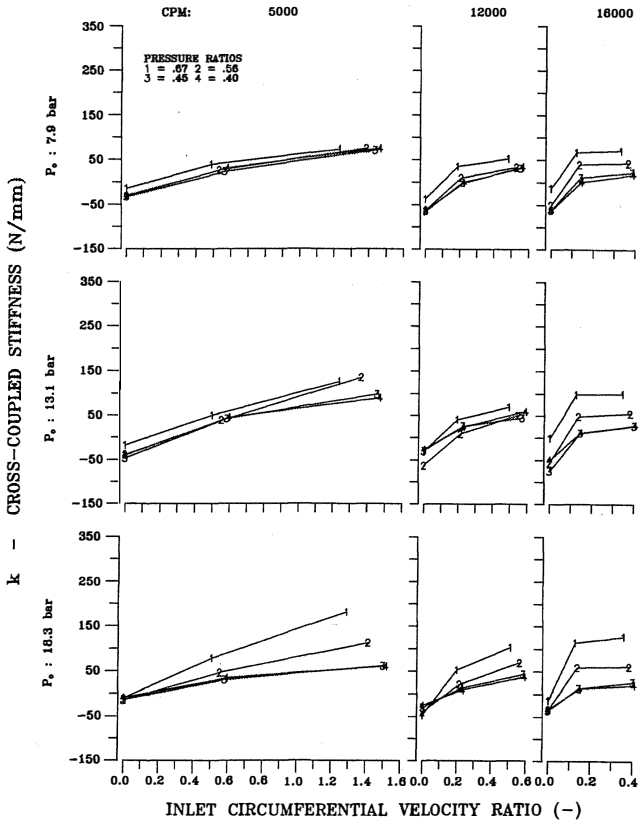

Figure 17. k vs $u_0(0)$ with Pressure Ratio as a Parameter for a TOS Seal, C_r/Rs = 0.003 [22].

Pelletti's [22] results concerning the destabilizing characteristics of TOS seals is consistent with the characterizations of unstable compressors by Kirk and Donald [23]. They considered 31 stable and unstable compressors, and concluded that compressors were more likely to be unstable as the following two parameters increase:

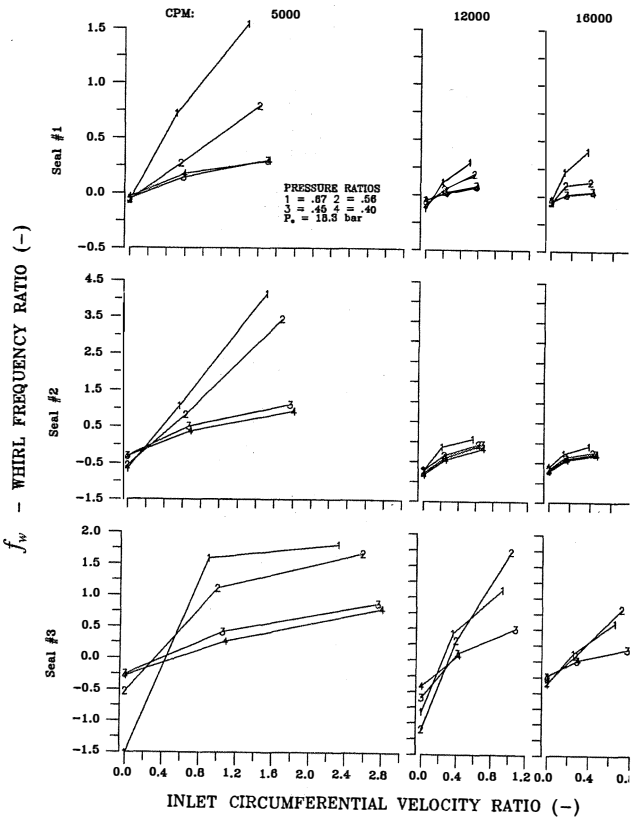

Figure 18. f_w vs $u_0(0)$ for a TOS Seal with Three Pressure Ratios C_r for Seals 1, 2, and 3 Are, Respectively, 0.003, 0.004, and 0.005 [22].

- The ratio of running speed to rotor critical speed ω/ω_n
- The product of compressor discharge pressure P_{dis} and ΔP

Their observation that compressors become less stable as the discharge pressure increases is consistent with Pelletti's [22] finding that labyrinths become more destabilizing as the pressure ratio across the seal increases.

Pelletti's [22] test results show that TOR labyrinths are modestly less stable than TOS seals. This result is intuitively reasonable since a TOS has a preponderance of stationary surfaces to slow the circumferential velocity of the gas in the seal, *vs* the TOR seal that has a preponderance of rotating surfaces. These results agree with the coastdown results cited earlier by Vance, et al. [21].

Hawkins, et al. [24], tested TOR labyrinths with honeycomb stators. The seals were tested in a noninterference fashion and accordingly, did not simulate an abradable seal operating geometry. Hawkins' [24] test results showed no reduction in measured values for k, with a honeycomb stator as compared to a smooth stator. His results were surprising, in that concurrent testing of smooth-rotor/honeycomb-stator seals (discussed later) showed a significant reduction in k. Kwanka [25] has recently reported similar results for honeycomb-stator/TOR seals.

Childs, et al. [26], presented test results for an interlocking labyrinth seal and found that this geometry had k values that were comparable to see-through labyrinths, but significantly lower values of damping. These results have not yet been explained in terms of CFD calculation but were quite repeatable.

Nelson, et al. [27], tested smooth seals with constant-clearance and convergent-taper geometry. Comparisons are shown in Figure 19 for f_w between a smooth constant-clearance seal, a see-through labyrinth, and a smooth-rotor/honeycomb-stator seal. The smooth seal is clearly most sensitive to preswirl, increasing linearly as $u_0(0)$ is increased. The authors have no direct experience in cases

where smooth seals were thought to cause an instability; however, the seals clearly have the potential to develop large values of k.

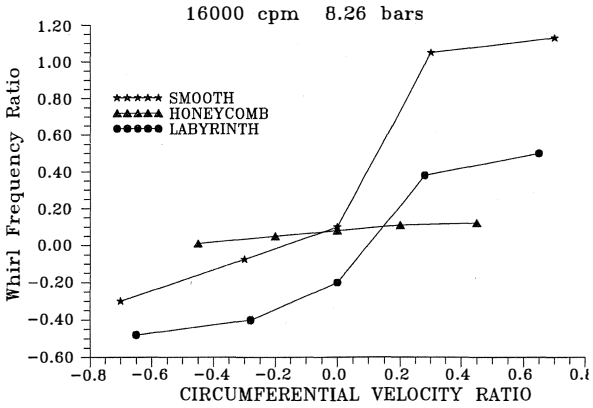

Figure 19. f_w vs $u_0(0)$ For: (A) a Smooth Constant-Clearance Seal, (B) a See-Through TOS Labyrinth, and a Smooth-Rotor-Honeycomb-Stator Seal [27].

Summarizing, labyrinth seals can create forces that are sufficient to destabilize a compressor or steam turbine. At the same operating conditions, see-through and interlocking seals have comparable k levels, but interlocking seals have lower values of damping. Honeycomb stators do not improve the rotordynamic characteristics of TOR labyrinths. TOS labyrinths are modestly more stable than TOR labyrinths. Smooth bushing seals can produce high levels of cross coupled stiffness coefficients. For labyrinth and smooth seals, the magnitude of destabilizing forces depends strongly on the level of preswirl of the gas approaching the seal.

IMPROVING ROTORDYNAMIC STABILITY THROUGH SEAL MODIFICATION OR REPLACEMENT

The preceding has covered seals that can degrade rotordynamic response. Our interest in this section concerns using annular seals to improve rotordynamic response, by either modifying or replacing existing seals. The options to be considered include swirl brakes, smooth-rotor/honeycomb-stator seals, brush seals, pocket damper seals, and shunt injection.

Swirl Brakes

Benckert and Wachter's [2, 15] successful implementation of swirl brakes was covered in the introduction. Childs and Ramsey [28] and Childs, et al. [29], have presented recent applications for swirl brakes. Pratt & Whitney is presently developing an alternate turbopump development (ATD) version of the high-pressure fuel turbopump (HPFTP) of the SSME. The ATD-HPFTP is similar to the currently manufactured HPFTP, using a three-stage fuel pump driven by a two-stage turbine. However, there are significant differences in the rotordynamics of the ATD-HPFTP and the HPFTP. From a gas-seal viewpoint, the ATD-HPFTP has a high pressure drop across the turbine-interstage seal, while the HPFTP does not. Also, the flow approaching the turbine-interstage seal is highly preswirled. The combination of a high-pressure drop and highly preswirled flow yielded a prediction, at the preliminary design stage, of an instability of the ATD-HPFTP due to the turbine-interstage seal. Pratt & Whitney elected to implement a swirl brake to guarantee stability of the turbopump.

Childs and Ramsey [28] tested a model of the Pratt & Whitney seal, and the seal and swirl-brake design are illustrated in Figures 20 and 21. A TOR abradable seal design is used with a honeycomb-lined stator. The approach velocity vector of Figure 21 does not have the correct flow angle, but merely indicates an approach velocity combining axial and circumferential components. The test seal has 145 individual vanes, with a pitch between vanes of 3.12 mm at their base radius of 7.42 cm. Each vane is 2.1 mm deep. The model did not have the same diameter or the same number of labyrinth cavities as the flight seal.

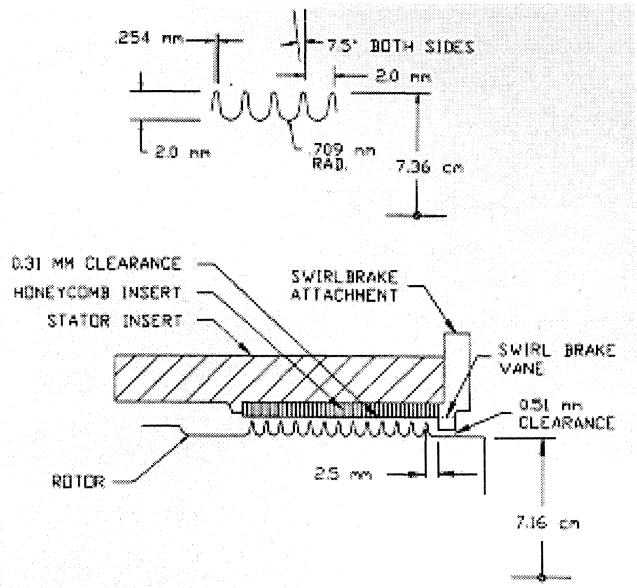

Figure 20. Model Seal Dimensions [28].

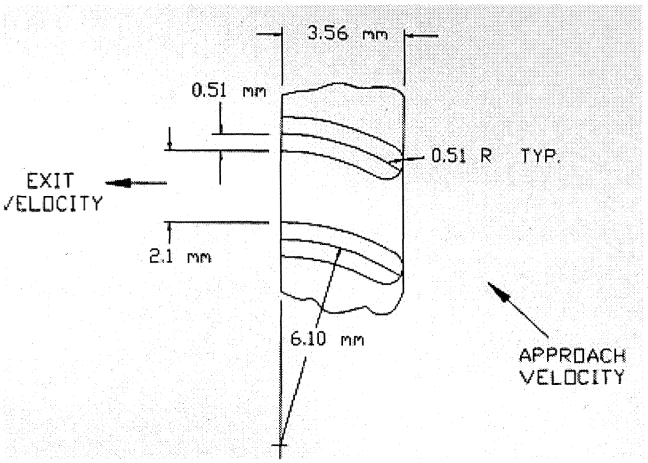

Figure 21. Swirl-Vane Geometry [28].

Illustrated in Figure 22 is k with and without the swirlbrake. The swirlbrake is seen to be highly effective, and the ATD-HPFTP has run to full speed and power without evidence of a rotordynamic instability.

The swirl-brake location is shown in Figure 23 for the turbine interstage seal of the SSME high pressure oxygen turbopump (HPOTP). In this case, the leakage gas moves inwards radially as it approaches the seal. As initially designed, the HPOTP used a stepped TOR labyrinth, and had serious synchronous and subsynchronous vibration problems. The initial attempted remedy for the problem involved replacing the TOR labyrinth with a smooth-rotor/honeycomb-stator seal. This change reduced, but did not eliminate, the subsynchronous component [30]. The next step toward a solution involved the addition of a swirl brake. The swirl-brake design that was implemented is shown in Figure 24. The initial design used radial slots. A proposed redesign in Figure 25 was expected to have improved aerodynamic capability for straightening the flow before it entered the seal. A comparison is provided in Figure 26 for k with the original and proposed redesign. The redesign was able to further reduce k by about 50 percent. These results suggest that an aerodynamic design is appropriate for swirl brakes; however, tests of a crude, nonaerodynamically

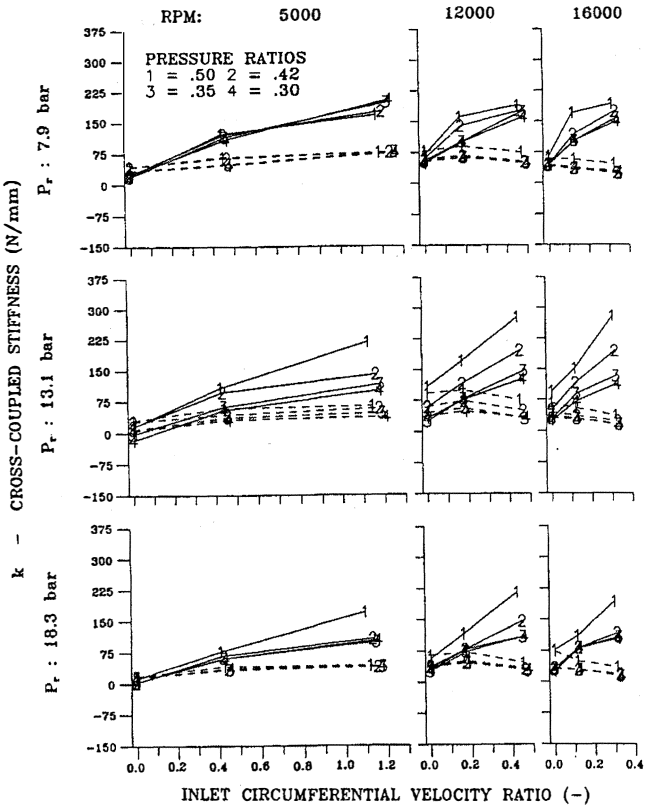

Figure 22. k vs $u_\theta(0)$ for the Test Seal with and without Swirl Brakes for Three Speeds, Three Supply Pressures, and Four Pressure Ratios [28]. (Dashed lines denote the seal with a swirl brake, solid lines without.)

designed swirl-brake for the Pratt & Whitney unit of Figures 19, 20, and 21, yielded lower values for cross coupled stiffness than the turning-vane design of Figure 20. Despite the superior model-test performance of the proposed redesign, for a variety of (good) reasons, the redesign was never tried in the HPOTP.

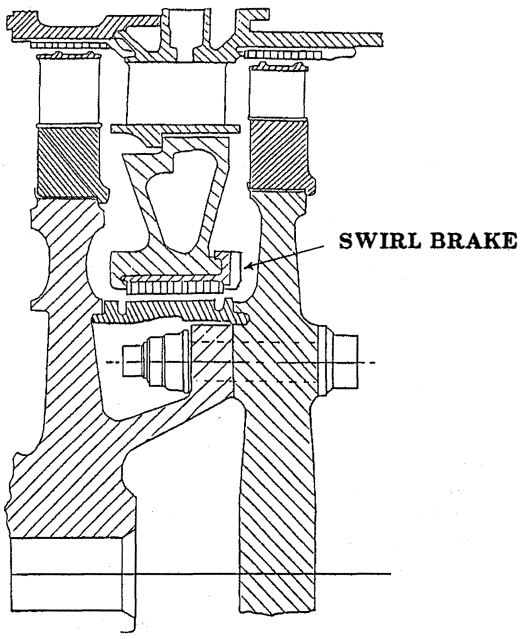

Figure 23. HPOTP Turbine Interstage Seal [29]. (Relative seal dimensions are not to scale.)

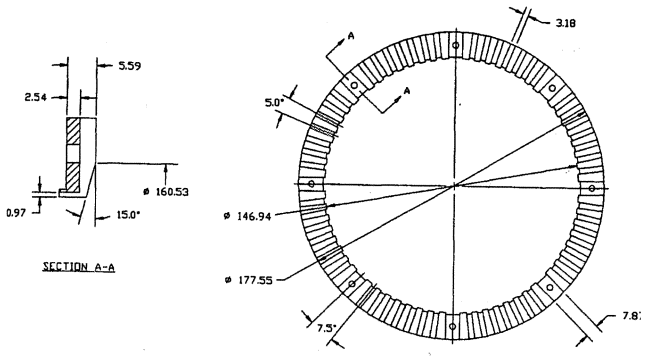

Figure 24. Current HPOTP Swirl-Brake Design [29].

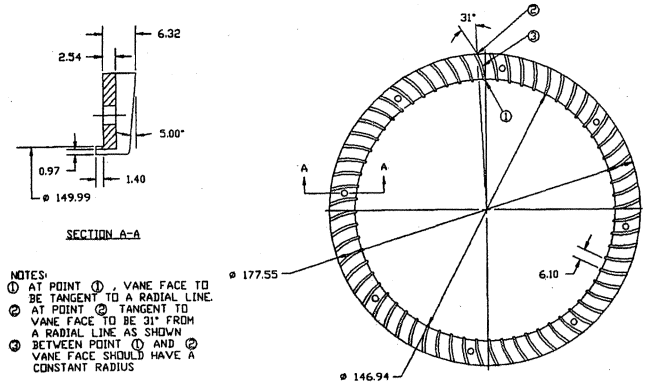

Figure 25. Proposed HPOTP Swirl-Brake Design [29].

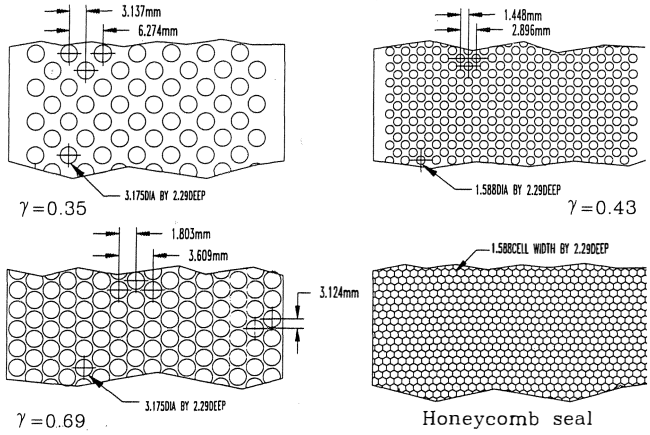

Figure 26. Surface Geometry for Gas Hole-Pattern Test Seals [36].

Smooth-Rotor/Honeycomb-Stator Seals

In this subsection, the term "honeycomb" will refer to smooth-rotor/honeycomb-stator seals. To the authors' knowledge, Rocketdyne's implementation of honeycomb seals was the first conscious attempt to improve rotordynamics by substituting a honeycomb seal for a labyrinth seal. The successful outcome brought support for a long study of honeycomb seals for the authors. Initial tests quickly confirmed that long (L > 2.54 cm (one inch) honeycomb seals leaked significantly less than TOR or TOS labyrinths, and also had *markedly* better rotordynamic performance. Despite impressive laboratory test results, users and manufacturers of commercial turbomachinery were initially cautious about implementing this technology. However, in recent years, many "success stories" have been published documenting honeycomb seals as an attractive remedy for unstable compressors. The initial report by Zeidan, et al. [11], was followed by Sorokes, et al. [31], and Gelin, et al. [32].

Test results by Kleynhans and Childs [33] showed that short (L = 2.54 cm (one inch)) honeycomb seals were not significantly better than TOS labyrinths. Hence, honeycomb-seal applications are generally only favorable for balance-piston seals, particularly for the center seal for back-to-back machines. Test results for longer (L > 5.05 cm (two inches)) honeycomb seals showed a consistent insensitivity to preswirl; hence, for these longer seals, swirl-brakes are generally not recommended.

Armstrong and Perricone [34] presented the first documented case-study of an unstable steam turbine that was fixed via retrofit of honeycomb seals. In this "steam-whirl" case, a 3600 rpm 30 MW machine was chronically unstable, such that it could not be operated comfortably above 19 MW. After retrofitting with honeycomb seals, the machine has been operated to 29 MW; however, current boiler limitations keep the machine from running above 23 MW. Circumferentially-segmented honeycomb was used in this application *vs* the normal compressor-application design that uses a single-unit construction.

Honeycomb seals can be manufactured with a variety of cell depths and cell widths. Aircraft gas turbines frequently use cell widths of 1/64th in (0.4 mm), while commercial machines more frequently use 1/32nd or 1/16th in (0.8 or 1.6 mm). Tests have shown good results for 1/16th (1.6 mm) cell widths and 0.125 in (3.18 mm) cell depth seals. "Dirty service" sometimes precludes the application of honeycomb because of concerns that, over time, the cells could be filled with deposits. The authors know of at least one case where clogging of the cells by dirty gas has occurred.

Some of the concerns that inhibit a wider application of honeycomb include structural failure of the braze joint in the seal construction, damage to the rotor during a rub event, and possible delays in having seals manufactured and installed. Benaboud, et al. [35], reported a structural failure of a honeycomb stator; however, recent applications of honeycomb seals at significantly higher ΔP's have not yielded any reported failures.

Putting aside concerns about shaft-damage during rub events for the moment, rubbing is less likely to happen with honeycomb seals than labyrinth seals because of much higher damping and potentially higher stiffnesses (more discussion on this point below). In addition, honeycomb seals are much tougher than labyrinths and will survive and function following surge conditions. The compressors discussed by Zeidan, et al. [11], generally became unstable (with labyrinths) after a surge event. They remained stable after surge events when retrofitted with honeycomb. Cases within the lab, where rubbing has occurred (inadvertently), have not caused serious shaft damage, as compared to rubbing against smooth aluminum seals that led to galling.

The authors were involved with an instability of six identical compressors that could not be taken off the test stand because of a rotordynamic instability. Initial calculations indicated that a honeycomb seal retrofit would solve the problem; however, the manufacturer could not get delivery of replacement honeycomb seal stators in less than six weeks. This delay was intolerable, and the problem was fixed with a pocket damper seal replacement. This case study is discussed below.

In response to the potential problems cited above, three "hole-pattern damper" gas seals were manufactured and tested [36]. Illustrated in Figure 26 are the three hole-pattern seal configurations and the competitive honeycomb pattern. In this figure,γ is the fraction of area taken up by holes. The $\gamma = 0.69$ pattern leaked less than the honeycomb seal and had better net damping characteristics. The seal stators were manufactured by a standard high-quality machine shop using a right-hand mill to make the holes. This design eliminates the braze-joint failure possibility and also reduces the manufacturing-delay-time worries. If the stator insert were to be made from a high-strength plastic, much of the shaft rub-damage worry would also disappear.

Progress in predicting rotordynamic coefficients for honeycomb seals did not proceed as well as their successful implementation into problem machinery. Nelson [37, 38] developed the first analyses using a "bulk-flow" model based on Hirs [39] turbulent lubrication approach. A bulk-flow model uses average axial and circumferential velocities across the (small) clearance and accounts for turbulence within the fluid *solely* with shear stresses at the rotor and stator surfaces. There is no radial variation in the pressure or velocity components in a bulk-flow model, and the shear stresses are defined in terms of friction factors. The rotor and stator friction factors are defined via bulk-flow Reynolds numbers relative to the wall. Nelson [37, 38] used a Blasius friction-factor model. Friction factors are the only difference between models for a smooth seal and a honeycomb seal. While Nelson's [37, 38] models gave reasonable results for smooth seals with constant-clearance or convergent-taper geometries, for honeycomb seals the correlation between measurement and predictions were never satisfactory.

Initial attempts that were made to improve Nelson's [37, 38] basic model concentrated on the entrance and exit regions [40, 41]; however, only modest improvements resulted. Subsequently, Ha and Childs [42] applied friction-factor data for honeycomb from flat-plate tests to Nelson's models with very limited success in improving predictions of rotordynamic coefficients.

In a discussion of their study, Ha and Childs [42] introduced the two-control-volume model of Figure 27. This model added control volume B for the gas in the honeycomb cells to the original (leakage flow-through) control volume A. Perturbed flow can enter control volume B in the radial direction; however, there is no flow in the axial or circumferential directions. Kleynhans and Childs [33] subsequently developed an analysis based on this model and found that the frequency-independent model of Equation (5) is basically wrong for most honeycomb-seal applications. Physically, the gas trapped in the honeycomb cells acts to *markedly* reduce the effective bulk modulus of the gas in the through-flow annulus (control volume A), which in turn reduces the effective acoustic velocity. As a consequence, the rotordynamic characteristics can be *strongly* frequency dependent.

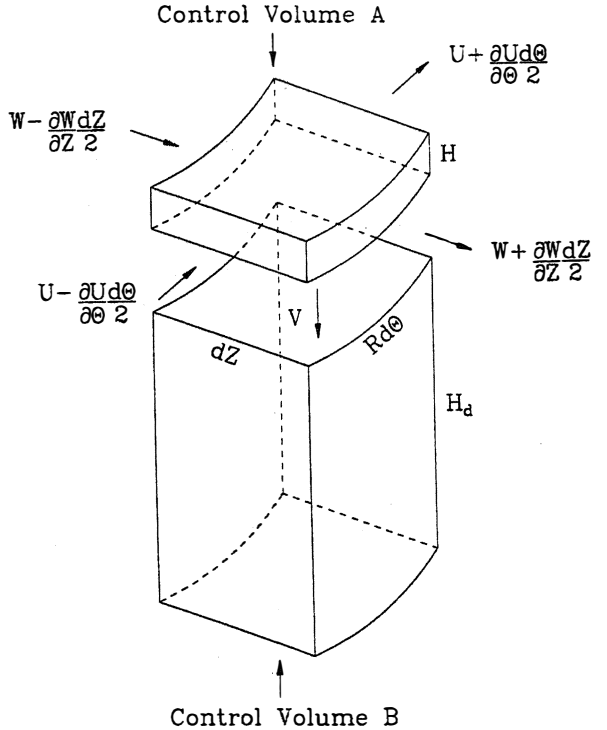

Figure 27. Two Control-Volume Model for Honeycomb Seals [33].

These results may explain why past comparison between measurements and experiments have been so consistently bad.

Specifically, comparisons have been made between:

- Test data for a strongly frequency-dependent seal
- Predictions for a frequency-independent model

Unfortunately, lab test data that are available for comparison are limited to a very narrow frequency range, 40 Hz to 70 Hz, *vs* the desired frequency range of 50 Hz to 500 Hz.

Kleynhans and Childs [33] developed the following frequency-dependent alternative model for honeycomb and hole-pattern gas damper seals:

$$-\begin{Bmatrix} F_x(s) \\ F_y(s) \end{Bmatrix} = \begin{bmatrix} D & E \\ -E & D \end{bmatrix} \begin{Bmatrix} x(s) \\ y(s) \end{Bmatrix} \tag{10}$$

where:

$$D(s) = \frac{K_D(s + \alpha)}{(s + \beta)} \tag{11}$$

and:

$$E(s) = \frac{K_E}{(s + \gamma)} \tag{12}$$

Illustrated in Figures 28 and 29 are effective (frequency-dependent), direct stiffness and damping coefficients corresponding to the D and E models of Equation (8) *vs* nondimensional frequency ($f = \Omega/\omega$) for various values of $h_d = H_d/C_r$ ratios, where C_r and H_d are the radial clearance and cell depth, respectively. Note that at the running speed ($f = 1$), increasing the hole depth increases the effective stiffness and decreases the effective damping.

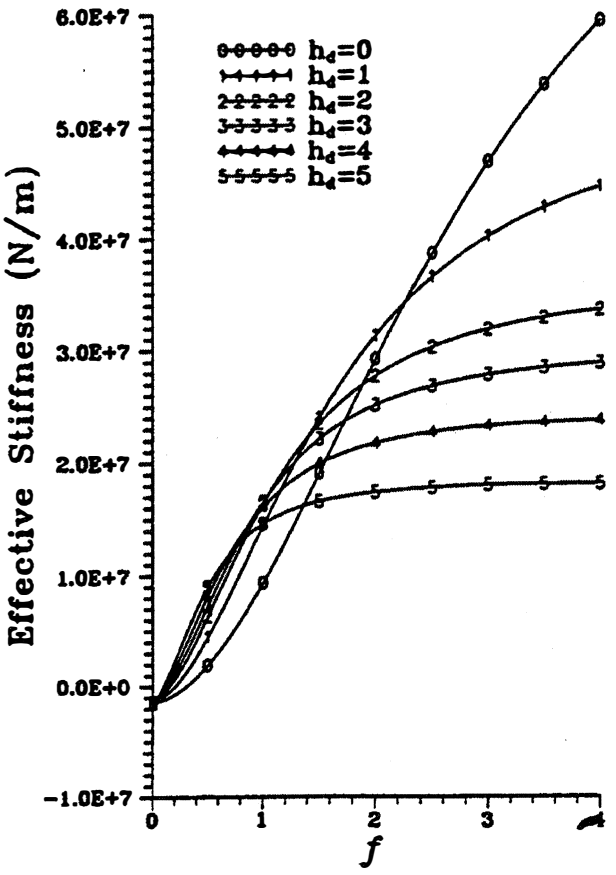

Figure 28. Effective Direct Stiffness vs *Normalized Frequency (f = ω/ω) for a Range of Normalized Hole Depths [33].*

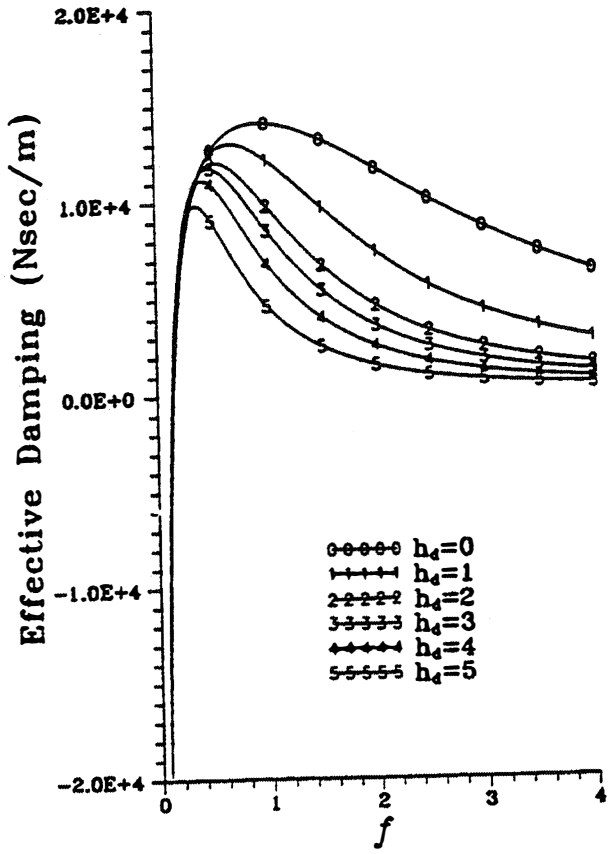

Figure 29. Effective Direct Damping vs *Normalized Frequency (f = ω/ω) for a Range of Normalized Hole Depths [33].*

The new model *predicts* much higher synchronous stiffness values for honeycomb seals than the earlier models, which is consistent with some observed shifts in critical speeds in retrofits of honeycomb seals. For high-pressure compressors, *predicted* stiffness values *at running speed* can be on the same order of magnitude as the bearings. If the predictions are correct, they open the possibility of adding stages to back-to-back machines. The validity of the predictions is the subject of a current, industrially-supported, research project. Frequency-dependent (50 Hz to 500 Hz) results are expected in about two years for comparison to the predictions.

Brush Seals

Conner and Childs [6] have presented the only published test data for brush seals. Provided in Figure 30 is a comparison between the cross coupled stiffness coefficients of an eight-cavity TOS labyrinth and a brush seal. k for the brush seal is negative and completely insensitive to preswirl. The measured damping values for brush seals are less than labyrinths; however, if a labyrinth is causing an instability, replacing it with a brush seal is likely to remedy the problem. ΔP restrictions are the primary limitation of brush seal application today. A single brush stage is good only for about 4.8 bars; higher ΔP's can permanently deform the brushes.

Shunt Injection

Shunt injection may have been initially used by some compressor manufacturers to control rotating stall *vs* improving rotordynamics. Criqui [43] cites shunt injection as an attractive means for restricting rotating stall, with a subsidiary benefit of eliminating preswirl to the balance-piston labyrinth. Memmott [44, 45] and Fozi [46] directly cite shunt injection as a means for eliminating instabilities. As stated earlier, shunt injection can be

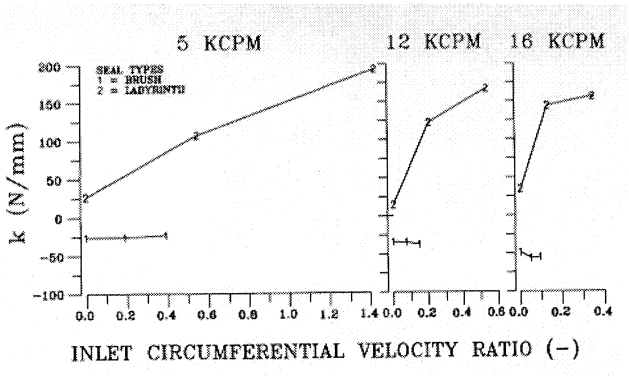

Figure 30. k vs $u_0(0)$ *for a Four-Stage Brush Seal and an Eight-Cavity TOS Labyrinth.*

either radial or against rotation. While widely used, until recent tests by Soto [47], no data have been presented demonstrating the effectiveness of shunt injection or comparing the performance of labyrinth seals using shunt injection to other seals. The radial-injection seal geometry tested by Soto [47] is presented in Figure 31. Note that the fourth tooth has been eliminated to provide room for injection. The labyrinth stator used for against-rotation injection is identical, except the injection angle is 30 degrees away from tangency. Comparisons are made between the injection labyrinths and a labyrinth without injection with and without preswirl, and a honeycomb seal. The noninjection labyrinth looked like Figure 31, except tooth four was not removed, and there were no injection holes. The honeycomb seal used a 1/16th in (1.58 mm) cell width and a 0.091 in (2.29 mm) cell depth. For all seals, L, D, and C_r were 2.5 in (63.5 mm), 5 in (127 mm), and 0.0087in (0.22 mm), respectively.

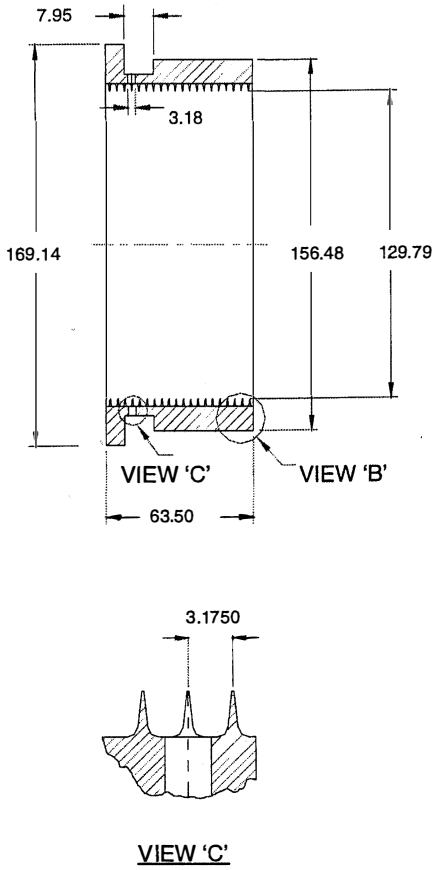

Figure 31. Test Labyrinth Seal with Radial Shunt Injection [47].

Depicted in Figure 32 is C_{eff} *vs* pressure ratio across the seal at 16,500 rpm. The supply pressure is 13.77 bars. The pressure ratio (PR) is the seal discharge pressure divided by the supply pressure. The injection pressure ratio (IPr) of 0.95 means that the injection pressure is 1/0.95 = 105 percent of the normal supply pressure of the seal. In terms of a compressor, this value would mean that the *compressor* discharge pressure is five percent greater than the pressure at the exit radius of the last impeller. Soto [47] also presents results for IPr = 0.9 and 0.85. Real compressors may have larger values for IPr (smaller injection over pressures). Soto had Mach numbers of 0.23 to 0.25 at the exit of the injection holes for IPr = 0.95.

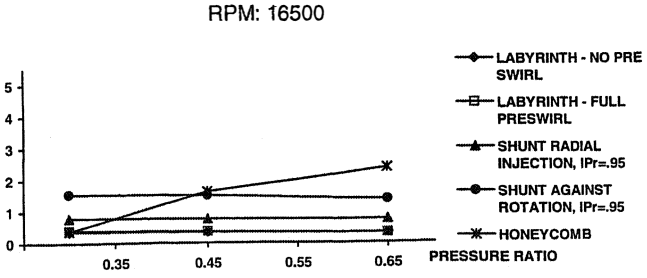

Figure 32. C_{eff} vs *Pressure Ratio for a TOS Labyrinth with Radial and Against-Rotation Injection and a Honeycomb Seal [47].*

With injection-against rotation, high values for C_{eff} are mainly developed from a negative value for k. C_{eff} decreases as running speed increases, because the shear flow from shaft rotation is growing stronger in comparison to the injected flow. The rotor surface speeds for the three speed cases of Soto [47] are 102 ft/sec (31.1 m/sec), 189 ft/sec (57.5 m/sec), and 360 ft/sec (110 m/sec).

In terms of real compressors, back-to-back compressors have pressure ratios across the center seal of 0.5 to 0.6, *vs* 0.4 to 0.5 for the balance-piston seal of through-flow machines. Surface velocities range from 328 ft/sec to 560 ft/sec (100 m/sec to 170 m/sec). Hence, Soto's [47] top-speed case is at the bottom end of the surface-speed range of real-compressors and is the only case with possibly direct relevance to real compressors. For the 16,500 rpm data set, injection-against rotation C_{eff} values are better than the honeycomb seal for PR less than about 0.4. For higher PR values, the honeycomb is better. Injection against rotation always yields greater values for C_{eff} than radial injection. Radial injection cases always gave higher C_{eff} values than the deswirled-entry cases (representing a labyrinth with 100 percent effective swirl brakes). Total mass flowrate through the injection seals was typically twice as large as the honeycomb leakage rate.

The decision to use (or not use) shunt injection needs to be made on a case-by-case basis, depending on the user's tolerance for increased leakage flowrate and the availability of adequate injection pressure. Soto's [47] results show that shunt injection can be quite effective if an adequate injection velocity can be achieved. In terms of field experience, the compressor discussed by Zeidan, et al. [11], was unstable with against-rotation shunt injection, but stable with honeycomb seals. Kanki, et al. [48], felt that against-rotation injection was very effective in stabilizing their compressor. Soto's [47] results clearly indicate the superiority of against-rotation injection over radial injection, providing that there is adequate injection pressure available.

Some manufacturers have chosen to continue using shunt-injection after replacing a labyrinth with a smooth-rotor/honeycomb-stator seal. Based on the available test data and experience with longer honeycomb seals, the authors know of no rotordynamic rationale in support of this practice. The rotordynamic coefficients of honeycomb seals with L > 2 in (50 mm) are insensitive to preswirl; hence, injecting gas to break up

the preswirl is not helpful. To the extent that shunt injection reduces the length of a long honeycomb seal, it reduces the effective direct damping and is counterproductive.

POCKET DAMPER SEALS

Optimum pocket damper seal designs tend to have fewer blades than conventional labyrinth seals, and smaller radial blade clearances. Requirements for rotordynamic damping must be balanced against the desire for low leakage. For a balance piston in a compressor, how the damping of this seal is sharply increased as the number of blades is reduced, is illustrated in Figure 33, and how the incremental reduction in leakage is diminished progressively as blades are added is shown in Figure 34. For several high pressure multistage centrifugal compressors such as the six stage application described below, four to six blades have turned out to be optimum as replacements for conventional seals that generally have twelve or more blades in the same axial length. The cross section of a typical six bladed version is shown in Figure 35. Notice that the blades are arranged in active pairs containing the separation walls to form the pockets. The annular space between the active pairs serves to equalize the pressure in preparation for entrance to the next downstream pair. This space is inactive, i.e. produces no damping by itself, so its axial length is made shorter than the active pockets.

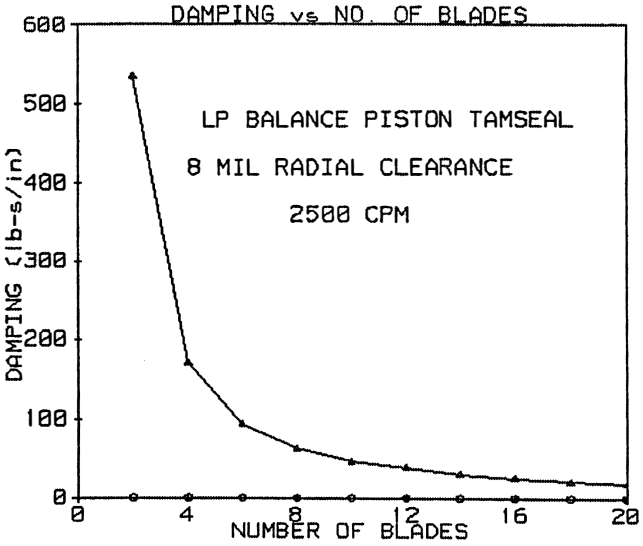

Figure 33. Damping of Constant Length Pocket Damper Seals vs *Number of Blades.*

Damping requirements must also be balanced against the requirement for sufficient seal clearance to avoid rubs, keeping in mind that a pocket damper seal will reduce the amplitudes of vibration and whirl. Also for a (different) balance piston, how the damping of this seal is increased as the blade clearance gets smaller, while the leakage is simultaneously reduced, is shown in Figures 36 and 37.

Laboratory testing of pocket damper seals has shown that the damping of two bladed versions is predicted fairly well up to pressure ratios of about 4.5 by the current code (Figure 38), while the damping of four bladed seals is overpredicted (Figure 39). The maximum damping for a given seal length is obtained with the minimum number of blades, which is two. Leakage measurements show about 30 percent more leakage than a conventional seal for the two bladed case (Figure 40), and about 14 percent more leakage for the four bladed case (Figure 41). These comparisons are for seals with the same number of blades, but, in most cases, a well designed pocket damper seal will have fewer blades than the conventional seal it replaces. The differences in leakage are due to

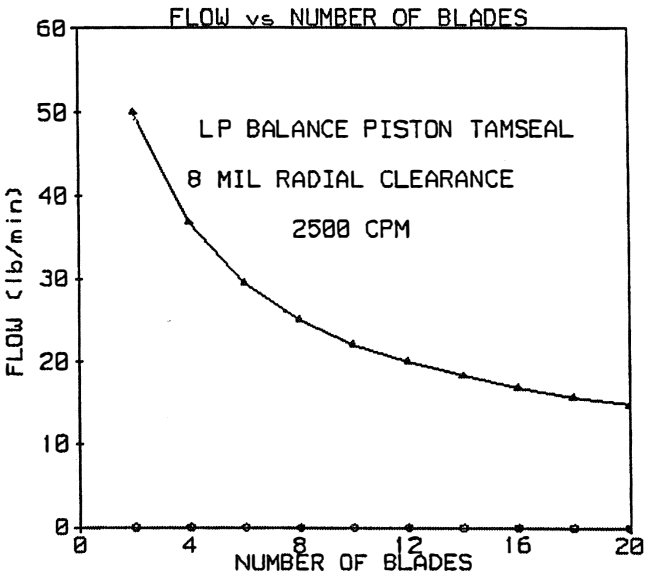

Figure 34. Leakage through Constant Length Pocket Damper Seals vs *Number of Blades.*

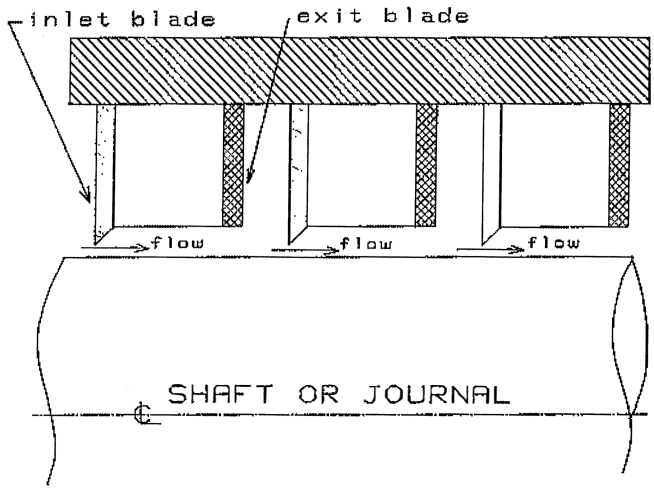

Figure 35. Conceptual Drawing of a Six Bladed Pocket Damper Seal Section with Exaggerated Clearances.

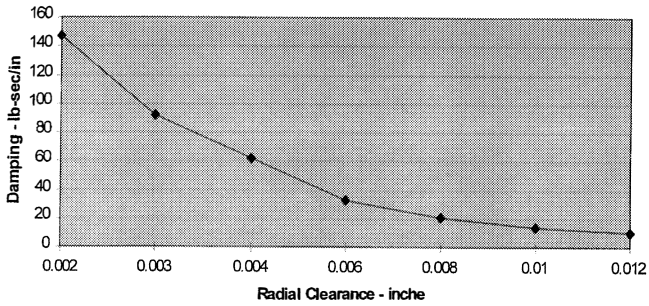

Figure 36. Damping of a Six Bladed Pocket Damper Seal vs *Clearance.*

the larger clearances of half the blades in this seal. Direct damping of a pocket damper seal depends on shaft motion producing less modulation of the leakage flow out of each pocket than the modulation of the leakage flow in. A newer variation of this seal (patent pending) accomplishes this by having all of the blades with the same clearance, but with small notches or holes in half the blades.

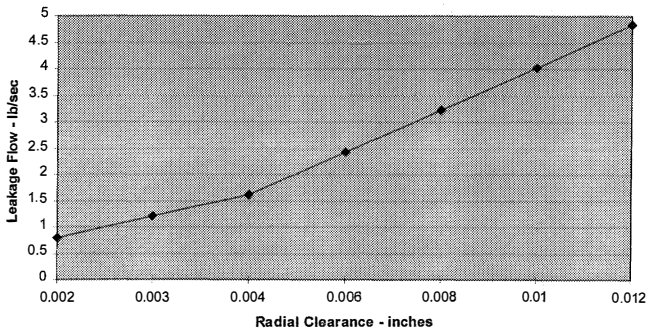

Figure 37. Leakage of a Six Bladed Pocket Damper Seal vs *Clearance.*

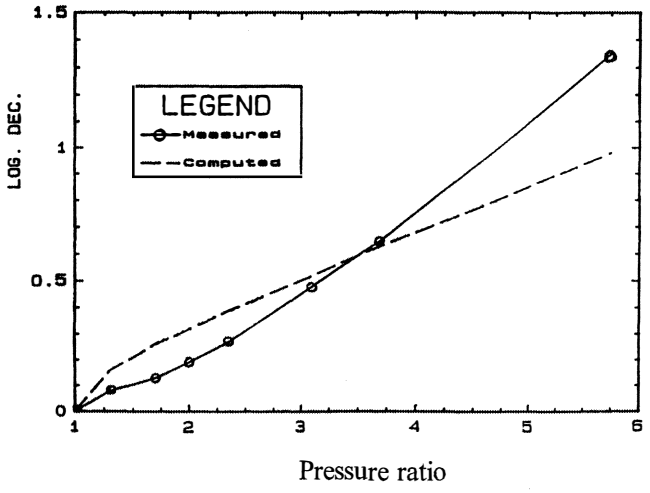

Figure 38. Measured and Computed Damping of the Prototype Two Bladed Pocket Damper Seal vs *Pressure Ratio.*

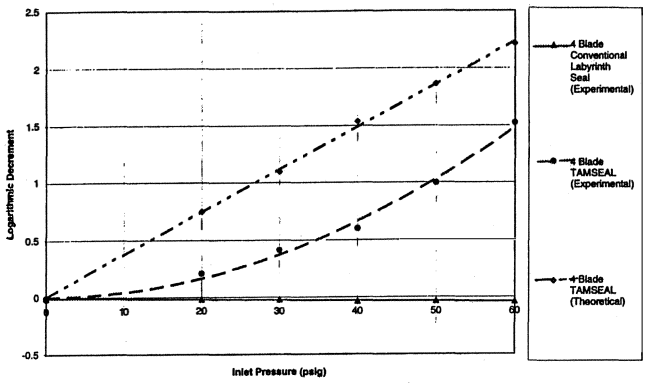

Figure 39. Measured Damping of a Four Bladed Labyrinth Seal (Bottom Line), and Damping of a Four Bladed Pocket Damper Seal (Measured, Middle Curve, and Theoretical, Top Line).

The great attraction of the pocket damper seal is in the very large direct damping obtainable, along with blockage of the gas swirl that produces cross coupled stiffness. An imbalance response measurement on a laboratory rest rig is shown in Figure 42 [49], which shows how a pocket seal (bottom trace) can completely eliminate the appearance of a critical speed. Logarithmic measurements from a laboratory test rig are shown in Figure 43 for a conventional labyrinth seal, a four bladed pocket damper seal with pockets shallower than optimum, and another seal with optimum depth pockets. Even the suboptimal damper seal has much more damping than the conventional seal (zero), but the optimum design has twice as much damping again. The optimum

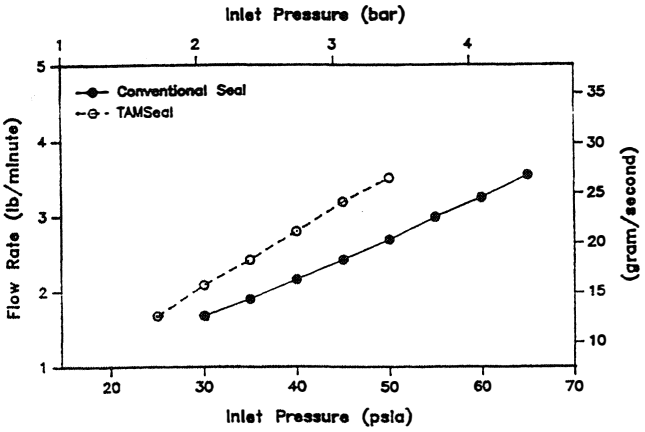

Figure 40. Measured Leakages of a Two Bladed Pocket Damper Seal and a Two Bladed Labyrinth Seal of Identical Length, Diameter, and Clearance.

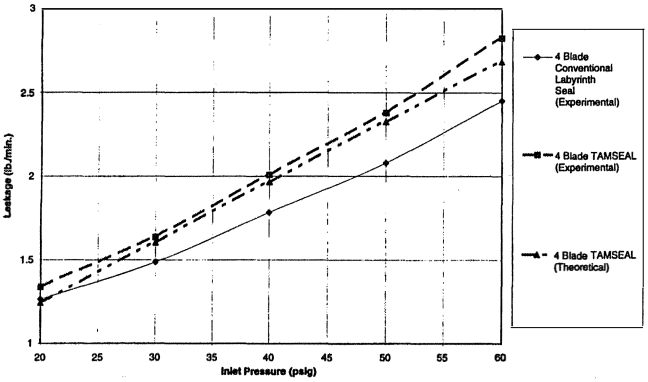

Figure 41. Measured and Computed Leakages of a Four Bladed Pocket Damper Seal (Top Two Lines) and a Four Bladed Labyrinth Seal of Identical Length, Diameter, and Clearance (Bottom Line).

pocket volume for each application is a function of the gas pressure and the frequency of the vibration to be damped. Also, depending on the application, the current computer code predicts a maximum high frequency where the damping begins to drop off sharply.

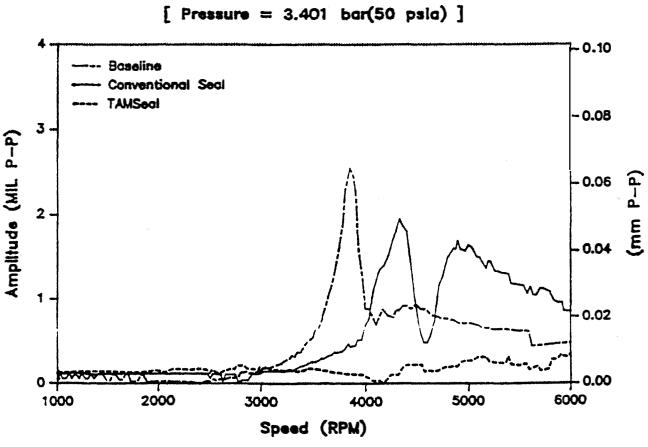

Figure 42. Imbalance Response Measured in Coastdowns on a Rotordynamic Test Rig with No Seal (Highest Peak), a Conventional Labyrinth Seal (Double Peak), and a Pocket Damper Seal (Bottom Curve) [49].

The best application for damper seals that the authors have seen to date is in multistage back to back compressors with center seals.

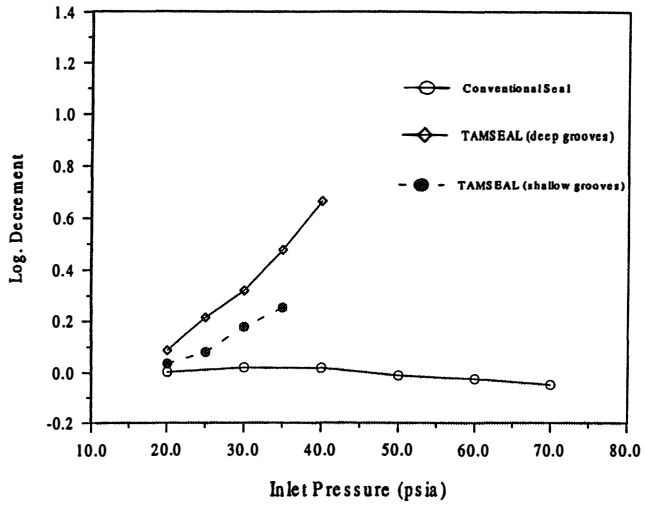

Figure 43. Measured Damping of a Four Bladed Pocket Damper Seal with Optimum Size Pocket Volumes (Top Curve), Pockets too Shallow (Middle Curve), and of a Conventional Labyrinth Seal of the Same Dimensions (Bottom Curve).

In the 1970s, the second author worked (for a consulting organization) on computer modelling a case that was rotordynamically unstable before damper seals were a reality. This case was later documented by publications in the literature [50, 51, 52]. Lund [53] published a paper in which one of his examples of stability analysis was remarkably similar to the subject case and may actually be the same one. Lund showed how difficult it was to achieve stability with damping in the bearings and remarked that "...an alternative method is to provide a damper which acts directly on the shaft. ...calculations have been performed with a damper bearing installed at the center of the rotor...the bearing is very efficient in stabilizing the rotor, but in practice it would be very difficult to provide a damper bearing at this location." Now, more than 20 years later and after invention of the trademarked pocket damper seal, the second author has extended his computer model of this compressor to show the effect of a damper *seal* at the center of the rotor to replace a seal that already resides there. It will be referred to in the figures and following text as the eight stage compressor.

Eight Stage Compressor

The design speed of this 22,000 hp compressor is 8500 rpm. It tripped out below the design speed repeatedly with subsynchronous whirl at a frequency of 4400 cpm, as load and speed were increased. The back-to-back layout of the eight wheels, shown in Figure 44, with 3140 psi (213.6 bar) pressure drop across the center seal at full load conditions. Using Wachel's empirical formula [52], to calculate the cross coupled stiffness at the impeller wheels, a rotordynamic computer model computes the logarithmic decrement as $\delta = -0.36$ (unstable), at a frequency of 4100 cpm when running at 7600 rpm. The mode shape is shown in Figure 45. Wachel's formula is based on his experience modelling centrifugal compressors and includes *all* sources of cross coupled stiffness in the compressor, including the seals.

Computed damping coefficients and leakage of a pocket damper seal retrofitted at the center labyrinth are shown in Figure 46 as a function of the number of blades fitted into the available axial length. The pressure drop of 3140 (214 bars) psi across the seal is so high, in this case, that the pocket damper seal can be designed with a large number of blades and it still produces enough damping to stabilize the compressor. Choosing the eight bladed damper seal gives a direct damping coefficient of C = 568 lb-s/in (99.5 N-s/mm). When this value is used at the center seal location, the rotordynamic computer code produces a computed logarithmic

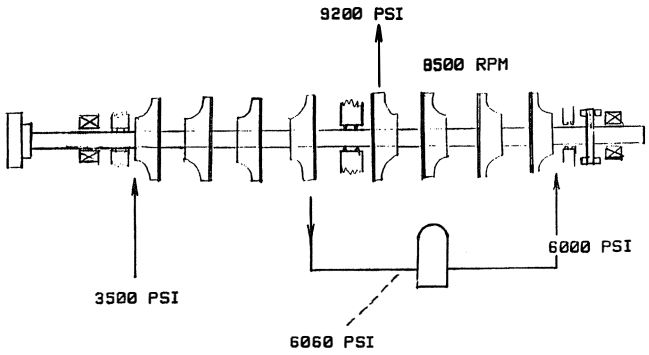

Figure 44. Pressures in the Eight Stage Compressor.

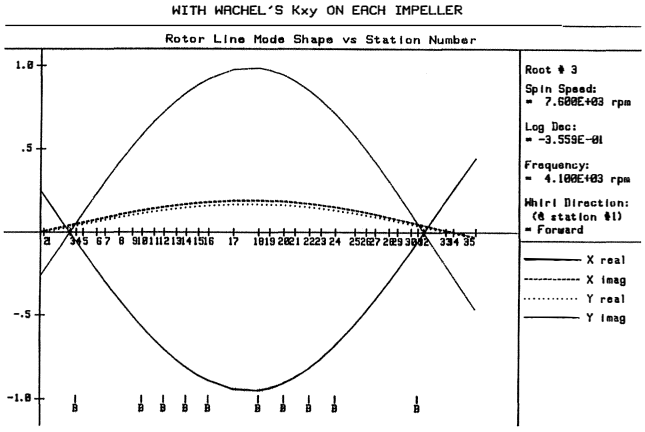

Figure 45. Computed Mode Shape of the Unstable Subsynchronous Rotor Whirl in the Eight Stage Compressor.

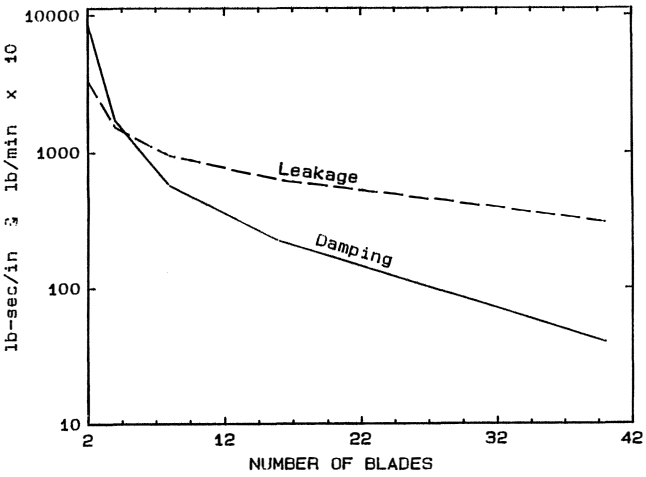

Figure 46. Computed Damping and Leakage vs *Number of Blades for a Pocket Damper Seal to Fit the Center Seal Location in the Eight Stage Compressor.*

decrement $\delta = 2.14$ (very stable). The 16 bladed damper seal gives C = 223 lb-s/in (39.1 N- s/mm) and $\delta = 0.57$ (stable).

Six Stage Compressor

After seeing the laboratory test results of the pocket damper seal at a consortium meeting of the laboratory, one engineer suggested the possibility of a field test in a centrifugal compressor that had a history of subsynchronous vibration problems [11]. This case involves a set of four back-to-back, six-stage machines that were originally installed on a platform in the

North Sea [54]. The second author computed damping coefficients for several pocket damper seal versions of a new center seal that could be retrofitted to the compressor, and also conducted a rotordynamic stability analysis of the expected results. The logarithmic decrement of the unmodified machine was predicted by the computer code to be −0.06 (unstable) and had a mode shape almost identical to Figure 45. The same mode was predicted to be very stable (3.1 logarithmic decrement) with a four bladed pocket damper seal. How the damping and the leakage are computed to vary with the number of blades in the damper seal is shown in Figures 47 and 48. Four blades were chosen as an optimum to achieve acceptable leakage with very high damping, since three identical sister compressors had proven difficult to stabilize in the past.

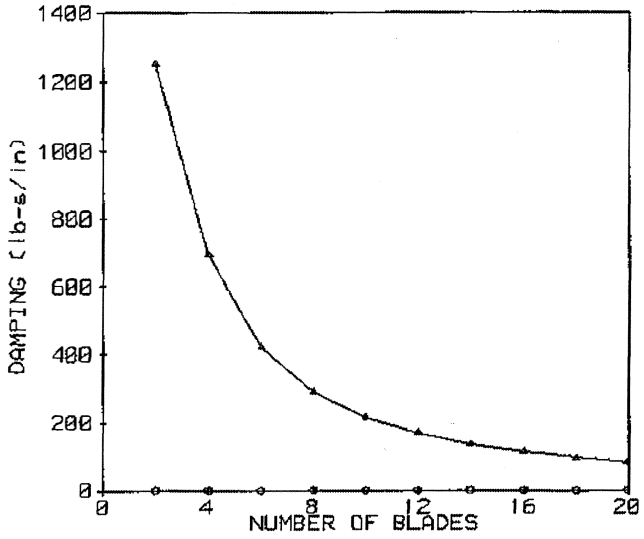

Figure 47. Compute Damping vs *Number of Blades for a Pocket Damper Seal to Fit the Center Seal Location in the Six Stage Compressor.*

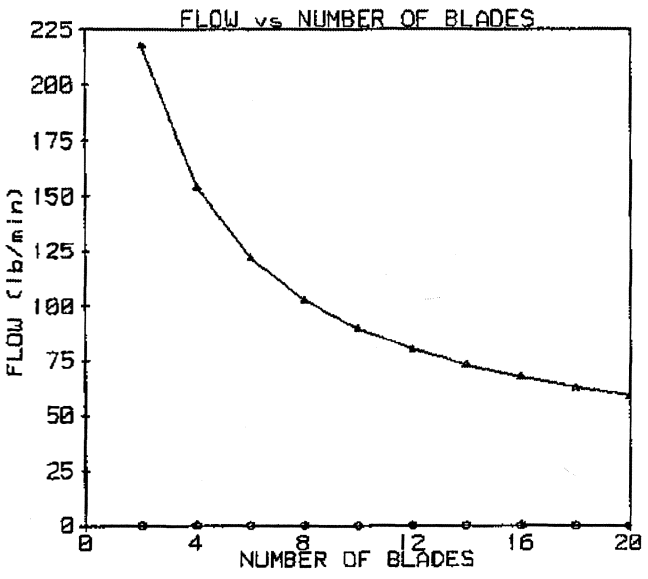

Figure 48. Computed Leakage vs *Number of Blades for a Pocket Damper Seal to Fit the Center Seal Location in the Six Stage Compressor.*

The subsynchronous vibration problem was eliminated through the use of the four bladed damper seal. The seal was constructed of TORLON™, a PAI material that is a high strength, high temperature engineering polymer (Figure 49). The labyrinth seals were split at the compressor horizontal joint to facilitate installation. This seal, by itself, produced acceptable stability in the machine, whereas the other three machines had been modified with honeycomb seals and squeeze film dampers. The use of the PAI material in the manufacture of the seals, their robust design, and careful engineering of tolerances and thermal properties, enabled the design of a seal that runs at closer clearances than conventional labyrinth seals. It has already been shown how smaller blade clearance produces more damping from the pocket damper seal design. This machine has had several full pressure surge events associated with emergency shutdowns since the installation of the pocket damper seal. There has been no observable degradation in the mechanical dynamic behavior of the machine due to those events, which is a very favorable contrast to the experience with these machines before modification.

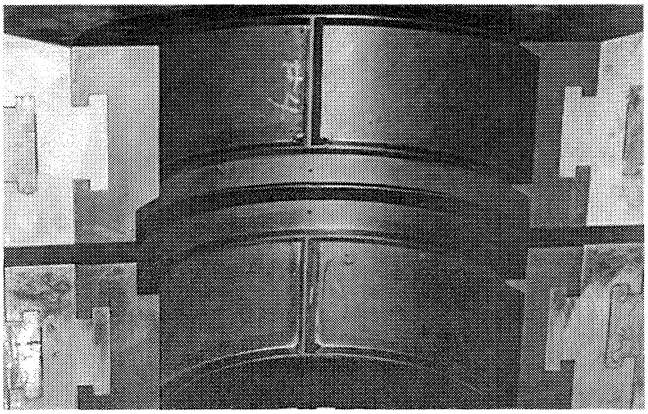

Figure 49. Split Half of the Pocket Damper Seal Installed in the Six Stage Compressor.

Steam Turbine

The pocket damper seals have not been installed in steam turbines to date, but the second author believes they should be a prime candidate to solve steam whirl problems. Consider the following example of retrofitting a labyrinth that seals steam at 670°F:

Rotor diameter D = 18 in (.457 m), Seal length L = 9 in (.229 m), Radial clearance C_r varies

Upstream pressure P_1 = 450 psi (30.6 bar), Downstream pressure P_2 = 350 psi (23.8 bar)

Whirl frequency to be damped Ω = 1800 cpm

The computed direct damping coefficient *vs* radial clearance for a four bladed pocket damper seal to fit this steam turbine application is shown in Figure 50. The cross coupled coefficient k is negligible. The effectiveness to damp an unstable whirl will depend on the axial location of the seal relative to the mode shape. Some locations could be four to 10 times more effective than the same amount of damping from the bearings.

Some steam turbine wheels have blade rims on the outer diameter with labyrinth seals. Recalling that the damping of a pocket damper seal is proportional to the product LD, it can be seen that very large damping coefficients could be obtained on wheels with a significant pressure drop.

Minimizing leakage is the reason why seals exist, and, even with damper seals, leakage is an important factor in choosing and optimizing the design. In labyrinth seals, the leakage is much more sensitive to radial blade clearance than it is to the number of blades. This fact carries over to be very important in optimizing the design of a pocket damper seal. Except for the hybrid brush/pocket damper seal

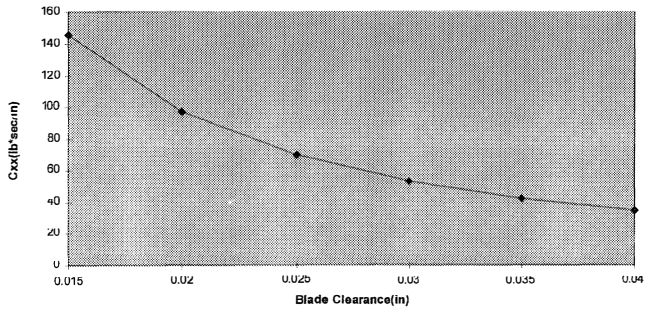

Figure 50. Computed Damping of a Pocket Damper Seal to Retrofit an 18 in Diameter Labyrinth in a Steam Turbine.

now under development, this seal will leak more than a conventional labyrinth seal with the same length and diameter, and with the same number of blades and the same minimum blade clearance. The damping obtainable from a pocket damper seal increases rapidly as the number of blades is *reduced*, while the seal length is held constant.

For turbomachines with rotordynamic problems, a damper seal can reduce the *actual* leakage by preventing seal rubs that open up the design clearance. Furthermore, reducing the radial clearance of a pocket damper seal, while holding the number of blades constant, increases the damping and reduces the leakage simultaneously. The radial clearance of labyrinth seals is usually chosen just large enough to avoid seal rubs with the expected amplitude of vibration or whirl. This has resulted in rules of thumb used by some manufacturers such as "two mils per inch of seal journal diameter." When rotordynamic amplitudes turn out to be larger than expected the result is seal rubs, along with actual leakage much larger than the design leakage on paper. In such cases the replacement of a conventional labyrinth seal with a pocket damper seal may produce an actual reduction in leakage, even though the leakage on paper is more. Concerns about seal rubs due to compressor surges and other transient events can be addressed, in some cases, by fabricating the pocket damper seal from a high strength resilient plastic, as shown in the six-stage compressor application discussed previously.

Low leakage is a major advantage of honeycomb seals, especially when the seal has axial sufficient length L. In choosing between honeycomb-stator/smooth-rotor seals and pocket damper seals to control rotordynamics, L is an important factor. For seals with $L \geq 50$ mm (two in), the honeycomb will have much less leakage, even less than a conventional labyrinth seal in many cases. For $L \leq 25$ mm (one in), a honeycomb seal has no better effective damping or leakage performance than a conventional labyrinth seal, and the pocket damper seal becomes the damper seal of choice. The pocket damper seal is the clear choice for eye-packing seals. A detailed comparison, including calculated leakage rates and calculated rotordynamic coefficients, is recommended for other applications.

The foregoing should not be interpreted to mean that short pocket damper seals produce more damping than long ones. Quite the contrary is true. The direct damping coefficient of one of these seals (with the number of blades held constant) increases directly with the projected area of its active pressure pockets, which depends on the product LD. Long pocket damper seals for high pressure compressors have been calculated by the second author to have direct damping coefficients in excess of 175,120 N-s/m (1000 lb- s/in).

For high pressure drops across the seal, the strength of the seal (resistance to axial blowout) may also become important, and the design of a pocket damper seal appears to offer more strength than a conventional labyrinth seal, due to its pocket separation walls.

SUMMARY AND CONCLUSIONS

The initial (narrow) view of labyrinth seals as "bad actors" that caused rotordynamic instability problems has broadened today, to the view that *annular* seals can be used to remarkably improve rotordynamic response and stability characteristics of turbomachinery. Reviewing, the known adverse results for interlocking and see-through labyrinths are as follows:

- Destabilizing forces developed by labyrinths are caused by fluid rotation within the seal. The fluid rotation can arise due to either fluid prerotation or be induced within the seal by shearing forces at the rotating shaft surface.
- Interlocking and see-through labyrinths have about the same level of destabilizing cross coupled stiffness coefficients k, but interlocking seals have lower levels of direct damping.
- Teeth-on-rotor (TOR) seals are modestly more destabilizing than teeth on stator (TOS) seals.
- Honeycomb stators are not effective in reducing k values for TOR labyrinth seals.
- The magnitudes of k values depends strongly on the level of gas preswirl at the seal entrance. Eye-packing and balance-piston seals normally have comparatively high preswirl values; shaft interstage seals normally have very low preswirl.

In terms of improving the behavior of an existing labyrinth, the following steps are available:

- Use swirl brakes—Properly designed swirl brakes can markedly reduce or eliminate k coefficients for labyrinth seals. They have been used successfully for axial and radial inflow seals. This approach is useful for eye-packing and balance-piston labyrinths.
- Use shunt injection—Provided the available injection pressure is adequate, shunt injection can be very effective in reducing k (radial injection) or reversing the sign (injection against rotation) for k. When properly designed (adequate injection velocity), against-rotation injection is much more effective than radial injection. Shunt injection will always have a performance penalty due to increased leakage flow.

Brush seals, honeycomb-stator/smooth-rotor seals, and pocket damper seals are the available choices for seal replacement to improve rotordynamic stability. The authors do not know of any cases where brush seals have been retrofitted to improve rotordynamic characteristics; however, they have negative or zero k values in combination with exceptionally low leakage. Present application for brush seals is limited by per-stage ΔP restrictions of around 70 psi (4.8 bars).

Honeycomb seals have been used to eliminate rotordynamic stability problems in several compressor applications and one documented steam turbine case. For $L \geq 1$ in (25 mm), honeycomb seals are no better than see-through labyrinth seals in terms of either leakage or rotordynamic characteristics. For $L \geq 2$ in (50 mm), honeycomb seals have excellent leakage and rotordynamic characteristics. Hence, long balance piston seals are the best potential application for honeycomb seals. "Dirty service" that could fill the cells over time is a concern in applying honeycomb. Rig tests have shown that seals with hole-pattern roughness designs for the stator can yield comparable performance to a honeycomb seal; however, this seal design has not yet been applied in a real machine. Analysis shows that honeycomb seals have strongly frequency-dependent stiffness and damping characteristics that can yield very high direct stiffness values at running speed. If confirmed by tests, this characteristic may be exploited in the future to add stages to back-to-back compressors.

Pocket damper seals block the swirl that produces cross coupled stiffness k and they produce large direct damping when ΔP is large enough (> 20 psi or 1.5 bars). They produce more damping than

any other type of gas seal when the axial length is short (< 1 in or 25 mm), but the damping increases with length, if the number of blades is held constant. The leakage is generally higher than for conventional labyrinth seals to fit the same application. The pocket separation walls have geometry that makes them stronger (to resist blowout) than other seal types of comparable dimensions. Pocket damper seals have been used to suppress subsynchronous whirl in several high pressure multistage centrifugal compressors and appear to be promising candidates for solving steam whirl problems.

In summary, annular seals represent remarkable possibilities to either improve or degrade the rotordynamic characteristic of high-performance turbomachinery. Readers who are interested in an alternative viewpoint on this topic may wish to consult Scharrer and Pelletti [55].

REFERENCES

1. Vance, J. and Schultz, R., "A New Damper Seal for Turbomachinery," ASME *60*, Vibration in Rotating Machinery, pp.139 (1993).
2. Benckert, H. and Wachter, J., "Flow Induced Spring Coefficients of Labyrinth Seals for Applications in Turbomachinery," Rotordynamic Instability Problems in High-Performance Turbomachinery, NASA CP2133, Proceedings of a workshop held at Texas A&M University, pp. 189-212 (1980).
3. Kirk, G., "A Method for Calculating Labyrinth Seal Inlet Swirl Velocity," Rotating Machinery Dynamics, *2*, ASME, pp. 345-350 (1987).
4. Dowson, P., Ross, S., and Schuster, C., "The Investigation of Suitability of Abradable Seal Material for Application in Centrifugal Compressors and Steam Turbines," *Proceedings of the Twentieth Turbomachinery Symposium*, Turbomachinery Laboratory, Texas A&M University, College Station, Texas, pp. 77-90 (1993).
5. Whalen, J., "The Use of Engineering Thermoplastics for Centrifugal Compressor Labyrinths," *Proceedings of the Twenty-third Turbomachinery Symposium*, Turbomachinery Laboratory, Texas A&M University, College Station, Texas, pp. 81-89 (1994).
6. Conner, K. and Childs, D., "Rotordynamic Coefficient Test Results for a 4-Stage Brush Seal," AIAA Journal of Propulsion and Power, pp. 462-465 (June 1993).
7. Chupp, R., Johnson, R., and Lowenthal, R., "Brush Seal Developments for Large Industrial Gas Turbines," AIAA 95-3146, Presented at the Thirty-first AIAA/ASME/SAE/ASEE Propulsion Conference (July 1995).
8. Greathead, S. and Bostow, P., "Investigations into Load Dependent Vibrations of the High Pressure Rotor on Large Turbo-Generators," Proceedings IMechE Conference on Vibrations in Rotating Machinery, Cambridge, England, pp. 279-286 (1976).
9. Kuehm, H., "Hawkins Inert Gas Plant: Design and Early Operation," Society of Petroleum Engineers, SPE 6793 (1978).
10. Fowlie, D. and Miles, D., "Vibration Problems with High Pressure Centrifugal Compressors," ASME Paper Number 75-Pet-28, Petroleum Engineering Conference, Tulsa, Oklahoma (September 1975).
11. Zeidan, F., Perez, R., and Stephenson, M., "The Use of Honeycomb Seals in Stabilizing Two Centrifugal Compressors," *Proceedings of the Twenty-second Turbomachinery Symposium,* Turbomachinery Laboratory, Texas A&M University, College Station, Texas, pp. 3-15 (1993).
12. Pollman, E. and Termuehlen, N., "Turbine Rotor Vibrations Excited by Steam Forces (Steam Whirl)," ASME Paper Number 75-WA/Pwr-11 (1975).
13. Thomas, H., "Instabile Eigenschwingungen von Turbinenläufern angefacht durch die Spaltströmungen Stopfbuschen und Beschauflungen," Bull de L'AIM, *71*, pp. 1039-1063 (1958).
14. Alford, J., "Protecting Turbomachinery from Self-Excited Rotor Whirl," Journal of Engineering for Power, pp. 333-344 (1965).
15. Benckert, H. and Wachter, J., "Flow Induced Spring Constants of Labyrinth Seals," IMechE, Proceedings of the Second International Conference, Vibrations in Rotating Machinery, Cambridge, England, pp. 53-63 (1980).
16. Childs, D., Elrod, D., and Hale, K., "Annular Honeycomb Seals: Test Results for Leakage and Rotordynamic Coefficients; Comparisons to Labyrinth and Smooth Configurations," ASME Transactions, Journal of Tribology, *111*, pp. 293-301 (April 1989).
17. Murphy, B. T. and Vance, J. M., "Labyrinth Seal Effects on Whirl Stability," Number C306-80, ImechE Proceedings, pp. 369-373 (1980).
18. Sundararajan, P. and Vance, J. M., "A Theoretical and Experimental Investigation of a Gas Operated Bearing Damper for Turbomachinery: Part 1—Theoretical Model and Predictions," ASME Transactions, Journal of Engineering for Gas Turbines and Power, *117*, pp. 742-749 (1995).
19. Iwatsubo, T., "Evaluation of the Instability Forces of Labyrinth Seals in Turbines or Compressors," NASA CP 2133, Workshop on Rotordynamic Instability Problems in High Performance Turbomachinery, Texas A&M University, College Station, Texas (May 1980).
20. Vance, J. M., *Rotordynamics of Turbomachinery*," New York, New York: John Wiley and Sons, pp. 131-133 (1988).
21. Vance, J. M., Zierer, J. J., and Conway, E. M., "Effect of Straight-Through Labyrinth Seals on Rotordynamics," Proceedings of the ASME Vibration and Noise Conference, Albuquerque, New Mexico (1993).
22. Kirk, G., "Labyrinth Seal Analysis for Centrifugal Compressor Design—Theory and Practice," Rotordynamics, Proceedings Second IFToMM International Conference on Rotordynamics, Tokyo, Japan, pp. 589-596 (1986).
22. Pelletti, J., "A Comparison of Experimental Results and Theoretical Predictions for the Rotordynamic Coefficients of Short (L/D = 1/6) Labyrinth Seals," M.S.M.E. Thesis, Texas A&M University and Turbomachinery Report Number TL-SEAL-1-90 (1990).
23. Kirk, G. and Donald, G., "Design Criteria for Improved Stability of Centrifugal Compressors," Rotor Dynamical Stability, ASME, pp. 59-72 (1983).
24. Hawkins, L., Childs, D., and Hale, K., "Experimental Results for Labyrinth Gas Seals with Honeycomb Stators: Comparisons to Smooth Stator Seals and Theoretical Predictions," ASME Transactions, Journal of Tribology, *111* (1), pp.161-168 (1988).
25. Kwanka, K., "Improving the Stability of Labyrinth Gas Seals," ASME IGTI Conference, Orlando, Florida (1997).
26. Childs, D., Elrod, D., and Hale, K., "Rotordynamic Coefficient and Leakage Test Results for Interlock and Tooth-on-Stator Labyrinth Seals," ASME Paper Number 88-GT-87, Gas Turbine Conference (June 1988).

27. Nelson, C., Childs, D., Nicks, C., and Elrod, D., "Theory Versus Experiment for the Rotordynamic Coefficients of Annular Gas Seals: Part 2—Constant-Clearance and Convergent-Tapered Geometry," ASME Transactions, Journal of Tribology, pp. 433-438 (July 1986).

28. Childs, D. and Ramsey, C., "Seal-Rotordynamic-Coefficient Test results for a Model SSME ATD- HPFTP Turbine Interstage Seal with and without a Swirl Brake," ASME Transactions, Journal of Tribology, pp. 198-203 (January 1991).

29. Childs, D. W., Baskharone, E. A., and Ramsey, C., "Test Results for Rotordynamic Coefficients of the SSME HPOTP Turbine Interstage Seal with Two Swirl Brakes," ASME Transactions, Journal of Tribology, 113, pp. 577-583 (July 1991).

30. Scharrer, J., discussion of the paper, "Annular Honeycomb Seals: Test Results for Leakage and Rotordynamic Coefficients; Comparison to Labyrinth and Smooth Configurations," by D. Childs, et al., ASME Journal of Tribology, *111*, pp. 293-301 (1989).

31. Sorokes, J., Kuzdzal, M., Sandberg, M., and Colby, G., "Recent Experiences in Full Load Full Pressure Shop Testing of a High Pressure Gas Injection Centrifugal Compressor," *Proceedings of the Twenty-third Turbomachinery Symposium*, Turbomachinery Laboratory, Texas A&M University, College Station, Texas, pp. 3-17 (1994).

32. Gelin, A., Pugnet, J., Bolusset, D., and Friez, P., "Experience in Full Load Testing Natural Gas Centrifugal Compressors for Rotordynamics Improvements," ASME Paper Number 96-GT-378, presented at the ASME Turbo Expo, Birmingham, United Kingdom (June 1996).

33. Kleynhans, G. and Childs, D., "The Acoustic Influence of Cell Depth on the Rotordynamic Characteristics of Smooth-Rotor/Honeycomb-Stator Annular Gas Seals," ASME Paper Number 96-GT-122, presented at the ASME Turbo Expo, Birmingham, United Kingdom (June 1996).

34. Armstrong, J. and Perricone, F., "Turbine Instability Solution—Honeycomb Seals," *Proceedings of the Twenty-fifth Turbomachinery Symposium*, Turbomachinery Laboratory, Texas A&M University, College Station, Texas, pp. 47-56 (1996).

35. Benaboud, N., Borchi, M., and Tesei, A., "Hassi R'mel High Pressure Injection Project with Centrifugal Compression," in Proceedings, Second European Congress on Fluid Machinery for the Oil, Petrochemical, and Related Industries, ImechE Conference Publication, pp. 167-176 (1984).

36. Yu, Z. and Childs, D., "A Comparison of Experimental Rotordynamic Coefficients and Leakage Characteristics Between Hole-Pattern Gas Damper Seals and a Honeycomb Seal," accepted for the 1997 ASME Gas Turbine Conference (1996).

37. Nelson, C., "Analysis for Leakage and Rotordynamic Coefficients of Surface-Roughened Tapered Annular Gas Seals," ASME Journal of Engineering for Gas Turbines and Power, *106*, pp. 927-934 (1984).

38. Nelson, C., "Rotordynamic Coefficients for Compressible Flow in Tapered Annular Seals," ASME Journal of Tribology, *107*, pp. 318-325 (1985).

39. Hirs, G., "A Bulk-Flow Theory for Turbulence in Lubricating Films," ASME Journal of Lubrication Technology, pp. 137-146 (1973).

40. Elrod, D., Nelson, C., and Childs, D., "An Entrance Region Friction Factor Model Applied to Annular Seals Analysis: Theory vs. Experiment for Smooth and Honeycomb Seals," ASME Journal of Tribology, *111*, pp. 337-343 (1989).

41. Elrod, D., Childs, D., and Nelson, C., "An Annular Gas Sea Analysis Using Empirical Entrance and Exit Region Frictior Factors," ASME Journal of Tribology, 112 (2), pp. 254-25 (1990).

42. Ha, T. and Childs, D., "Annular Honeycomb-Stator Turbulen Gas Seal Analysis Using New Friction-Factor Model Based or Flat Plate Tests," ASME Journal of Tribology, *116*, pp. 352-360 (1994).

43. Criqui, A., "Advancements in Gas Compressor Stability,' Turbomachinery Technology Seminar, Solar Turbines Incorporated (1986).

44. Memmott, E. A., "Tilt Pad Seals and Damper Bearing Applications to High Speed and High Density Centrifuga Compressors," Proceedings of the Third IFToMM International Conference, Lyon, France, pp. 585-590 (1990).

45. Memmott, E. A., "Stability of Centrifugal Compressor by Application of Tilt Pad Seals, Damper Bearings, and Shun Holes," Proceedings of the Fifth International Conference or Vibrations in Rotating Machinery ImechE, Bath, England, pp. 99-108 (1992).

46. Fozi, A. A., "An Examination of Gas Compressor Stability and Rotating Stall," Rotordynamic Instability Problems in High Performance Turbomachinery, NASA CP 2443, Proceedings of a Workshop held at Texas A&M University, College Station, Texas, pp. 19-33 (1986).

47. Soto, E., "Experimental Rotordynamic Coefficient Results for (a) a Labyrinth Seal with and without Shunt Injection, and (b) a Honeycomb Seal," M.S. Thesis, Texas A&M University (1997).

48. Kanki, H., Katayama, K., Morii, S., Mouri, Y., Umemura, S., Ozawa, U., and Oda, T., "High Stability Design for New Centrifugal Compressor," Rotordynamic Instability Problems in High Performance Turbomachinery, NASA CP 3026, Proceedings of a Workshop held at Texas A&M University, College Station, Texas, pp. 445-459 (1988).

49. Vance, J. M. and Li, J., "Test Results of a New Damper Seal for Vibration Reduction in Turbomachinery," ASME Transactions, Journal of Engineering for Gas Turbines and Power, *118*, pp. 843-846 (October 1996).

50. Cochrane, W. W., "New-Generation Compressors Injecting Gas at Ekofisk," The Oil and Gas Journal, pp. 63-70 (May 1976).

51. Doyle, H. E., "Field Experiences with Rotordynamic Instability in High Performance Turbomachinery," NASA CP133 Proceedings of a Workshop held at Texas A&M University, College Station, Texas, pp. 3-13 (1980).

52. Wachel, J. C., "Rotordynamic Instability Field Problems," NASA CP2250 Proceedings of a Workshop held at Texas A&M University, College Station, Texas, pp. 1-19 (1982).

53. Lund, J. W., "Stability and Damped Critical Speeds of a Flexible Rotor in Fluid Film Bearings," ASME Transactions, Journal of Engineering for Industry, *96*, pp. 509-517 (1974).

54. Richards, R. L., Vance, J. M., Paquette, D. J., and Zeidan, F. Y., "Using a Damper Seal to Eliminate Sybsynchronous Vibrations in Three Back to Back Compressors," *Proceedings of the Twenty-fourth Turbomachinery Symposium*, Turbomachinery Laboratory, Texas A&M University, College Station, Texas, pp. 59-71 (1995).

55. Scharrer, J. and Pelletti, J., "Leakage and Rotordynamic Effects of Compressible Annular Seals, *Proceedings of the Twenty-fourth Turbomachinery Symposium*, Turbomachinery Laboratory, Texas A&M University, College Station, Texas, pp. 175-190 (1995).